

Dear Editor,

We provided the replies to the comments as follows, with referring to the probable changes in the revised manuscript. In addition to the changes from reviewers' comments, we removed Figures 1 and 10. Moreover, we removed Figures 8 and 9 and table 6 (comparing to the Budyko curves), because we evaluated our results through the Budyko framework, as suggested by Stephen Good. Accordingly, any explanations in the text related to these figures and table were also removed. These changes are shown in the manuscript by track changes.

Reviewer 1 (Stephen Good):

General Assessment

Comment 1:

This modeling and analysis are conducted in a satisfactory manner. However, it is hard to see how yet one more model that estimates evapotranspiration subcomponents moves us closer to a better understanding of these fluxes.

Reaction:

Our aim is not to provide yet another LSM that partitions evaporation. Our aim is to show with a simple analytical model that the Budyko framework can be explained. For this we use the reasoning of the Gerrits model that recognizes the characteristic time scales of the different evaporation processes (i.e. interception daily and transpiration monthly). We revised the Gerrits model in such way that it was possible to apply it at the global scale. As suggested by the reviewer, we clarified this better and related the results of the model to the Budyko framework for a better understanding the partitioning of evaporation into transpiration and interception. For this paper, we changed the introduction for better explanation of our aim. Moreover, we provided Figures 7, 8 and 9 in the revised manuscript for better understanding of the evaporation partitioning through the Budyko framework.

Comment 2:

The introduction and a paragraph in the discussion relate this model to the Budyko framework. One possible way forward for the authors is evaluating how trends in flux components relate the energy and water limitations outlined by the Budyko framework, since this is the stated motivation of this model. This could move the paper beyond how it is currently presented as another land surface model applied using remote sensing observations. For example, see Figure 11 of Miralles's 2016 HESS paper for casting total evaporative fluxes in this context. Also relevant is the study of Good (Nature Ecology & Evolution 2018) which used a Budyko approach to examine how to partition evaporative fluxes. In revising the paper, I suggest the authors work to find how this approach helps us understand the different surface to atmosphere water flux pathways better.

Reaction:

We thank the reviewer for this valuable suggestion. We agree that our aim was not clearly defined and also misleading in that sense. As suggested by the reviewer, we evaluated the relation between evaporation fluxes and energy/water limitation in Budyko framework as provided by Miralles et al. (2016) and Good et al. (2017). As mentioned in reaction to comment 1, we provided Figures 7, 8 and 9 in the revised manuscript for each land cover, and for the evaporation fluxes (E_i and E_t and E_{tot}), separately, to discuss how our model can be related to the Budyko framework.

Comment 3:

Most critically, I find the language in this paper to be grandiose and predicated on a poorly based argument. As is written in the abstract and introduction, the authors suggest that others have “tried to improve the Budyko framework by including more physics and catchment characteristics... However this often resulted in additional parameters, which are unknown or difficult to determine.” This statement, and others like it in this paper, is inappropriate for two reasons: (1) other approaches have used fairly easy to measure characteristics and (2) because the authors proceed to do exactly what they claim shouldn’t be done by fitting “difficult” to determine parameters to optimize their results. For point (1) for instance, the approach of Porporato is explicitly physically based as is it dependent on the ratio soil water storage to mean rainfall depth which is a measurable quantity. Furthermore, both of these quantities are used in the analysis presented here. For reason (2), the ‘b’ parameter of this analysis, among others, is clearly stated by the authors (P5L15) to have been calibrated to produce the best results. This is very similar to the Li (WRR 2013) paper wherein the Budyko curve parameters were fit to vegetation cover. The authors use of language such as “tried” (P2L18) seems to imply these other authors were unsuccessful, which may not be true. In my opinion, this submitted paper is quite similar to these other efforts in that it has extended the Budyko framework with new parameters they have fitted based on physical processes. Here, the most important parameters dictating the transpiration component are when transpiration becomes downregulated, and how much maximal transpiration can be. Equation 17 needs more elaboration and justification, as does the parameterization of S_b as 50% of $S_{u,max}$. How were these values selected and what is the consequence of other using other values here. How much do these choices, and other values such as the ‘b’ parameter, influence model outcomes.

Reaction:

Yes, you are right that we also have some calibration parameters. Thus, we rephrased our text. Nonetheless, we think that we use a slightly different approach for these calibration parameters and other model parameters as well. Although others indeed also use ‘measurable parameters’, which could be tested in some case studies, some of these input values are not available at the global scale such as for example the soil water storage. For example, carry over parameter (A) was available for 10 locations in Gerrits et al. (2009), but at global scale we did not have such data, so we proposed $A=b*S_{u,max}$, and we need to calibrate the “b” parameter to link A to a measurable variable. About the S_b as 50% of $S_{u,max}$, we mentioned in the text that in this study we assumed S_b to be 50% of $S_{u,max}$, as this value is commonly used for many crops, referred

to (Allen et al. 1998). However, we provided a sensitivity analysis in the revised which shows that the model is not sensitive to this parameter for none of the land covers.

Specific Comments:

Comment 4:

P1L11: The $1/(1+f(\phi))$ is not the base of all Budyko curves. Budyko, himself used a hyperbolic tangent as an example. What do the lower and upper case f's represent?

Reaction:

As mentioned by Arora (2002), evaporation ratio (E/P) is a function of the aridity index (Φ) and Bowen ratio (γ) ($\frac{E}{P} = \frac{\Phi}{1+\gamma}$). Arora interpreted the equation as follows:

“As a region becomes dry and is characterized by high potential evaporation, low precipitation and evapotranspiration, and high sensible heat fluxes then $\Phi \rightarrow 1$, $\gamma \rightarrow 1$ and E/P tends towards unity implying little runoff. the other hand, as a region becomes wet and is characterized by low values of aridity index (Φ) and Bowen ratio (γ) then $E/P < 1$ and runoff occurs. Since Bowen ratio (γ) is also a function of available energy and precipitation (and thus a function of Φ) evaporation ratio may be expressed as a function of aridity index alone.” It leads to equation 1 in our paper. Thus, in equation 1, f and F are both mathematical functions, showing that E/P is a function of the aridity (Φ). $F(\Phi)$ can have many forms (exponential, hyperbolic tangent, etc.) as summarized in Table 1.

Comment 5:

P2L33: This paper estimates available soil water capacity, not the actual soil water itself. Also, I wouldn't call these 'data' but modeled estimates.

Reaction:

Gao et al. (2014) presented a new method where the available soil water is derived from time series of rainfall and potential evaporation, plus a long-term runoff coefficient. We agree that knowing soil moisture storage change is important for the Budyko framework, but we use a method whereby we work around it by using plant available water. The method of Gao et al. (2014) provides plant available water (which is often linked to soil water capacity). In our paper we used it as $S_{u,max}$. We rephrased it in the manuscript to explain it more precisely.

Moreover, “data” refers to rainfall, potential evaporation and runoff coefficient which is used by Gao et al. (2014) to estimate the available soil water. However, we changed “data” into “**input time series**”.

Comment 6:

P3L16: Evaporation from ‘non-superficial’ soil moisture

Reaction:

Thanks. We added this.

Comment 7:

P4L11: Do you mean daily, not yearly, average.

Reaction:

Yes, daily average during the year. We corrected it in the text.

Comment 8:

P5L14: I think you should also place these eqn in table 2 for consistency: $A = b \cdot S_{u,max}$ as well as $S_b = 0.5 \cdot S_{u,max}$

Reaction:

Ok, these equations moved to table 2 (equations 8 and 18, in the revised manuscript).

Comment 9:

P5L36: Reword here. As is stated above and in eq17, you do not hold $D_{t,m}$ constant? Which is it?

Reaction:

We keep $D_{t,m}$ constant during the year (like $D_{i,d}$), but equation 17 shows that we calculated it as a function of the average yearly LAI. For water-constrained areas this is not a problem, because there $E_{t,m}$ is determined by the LHS of the min-function ($A + B(P_m - E_{i,m})$) as can be seen in Equation 7. For energy-constrained areas our assumption can be problematic. However, in those areas often temperature and radiation follow a sinusoidal pattern without complex double seasonality as e.g., occurs in the ITCZ. This implies that the overestimation of $E_{t,m}$ in winter will be compensated (on the annual time scale) by the underestimation in summer time.

Comment 10:

P5L38: Do you have a justification or citation for this statement?

Reaction:

Please see our response to comment 9.

Comment 11:

P7L17: No observations were used here. Only comparisons of the Gerrits model against other models.

Reaction:

It is a general sentence for Taylor diagram, not only for our model. But to make it clear, we changed "This diagram can provide a concise..." into 'A Taylor diagram can provide a concise...'

Comment 12:

P8L42: There are many bare soil estimates (See the review by Kool 2014 Agg and Forest Met, for example).

Reaction:

We meant that there is hardly any data on the forest floor interception storage capacity (S_{max}). We did not intend to refer to bare soil evaporation.

Comment 13:

F2: Because of the size of these figures, and the large range of values, it becomes hard to discern differences. Why not plot the absolute value of E flux in panel A, and then the differences in panels B, C, and D. Consider this approach in later figures as well

Reaction:

Thanks for your suggestion. We did it before, but the single pixel outliers may blow up the entire figure what was also not a good way of showing the differences. That's why we moved towards the Taylor diagrams. Moreover, we also wanted to show the original data.

Comment 14:

F3: Units for the RMSE, here and onward.

Reaction:

We used normalized RMSE in these figures as shown in the following equation, so it has no unit.

$$\text{NRMSE} = \frac{\text{RMSE}}{\overline{X_0}} \quad (1)$$

In this equation, NRMSE is normalized RMSE and $\overline{X_0}$ is the average of observation values (here the values estimated by Gerrits' model).

References

- Allen RG, Pereira LS, Raes D, Smith M (1998) Crop evapotranspiration-Guidelines for computing crop water requirements-FAO Irrigation and drainage paper 56. FAO56, Rome
- Arora VK (2002) The use of the aridity index to assess climate change effect on annual runoff. *J Hydrol* 265:164–177. doi: 10.1016/S0022-1694(02)00101-4
- Gao H, Hrachowitz M, Schymanski SJ, et al (2014) Climate controls how ecosystems size the root zone storage capacity at catchment scale. *Geophys Res Lett* 41:7916–7923. doi: 10.1002/2014GL061668
- Gerrits AMJ, Savenije HHG, Veling EJM, Pfister L (2009) Analytical derivation of the Budyko curve based on rainfall characteristics and a simple evaporation model. *Water Resour Res* 45:W04403. doi: 10.1029/2008WR007308
- Good SP, Moore GW, Miralles DG (2017) A mesic maximum in biological water use demarcates biome sensitivity to aridity shifts. *Nat Ecol Evol* 1:1883–1888. doi: 10.1038/s41559-017-0371-8
- Miralles DG, Jiménez C, Jung M, et al (2016) The WACMOS-ET project - Part 2: Evaluation of global terrestrial evaporation data sets. *Hydrol Earth Syst Sci* 20:823–842. doi: 10.5194/hess-20-823-2016

1 **Reviewer 2:**

2

3 **Comment 1:**

4 **Equation (3b): $E = E_i + E_t$. Since E_i includes soil evaporation, I would suggest to interpret this as**
5 **$ET = E + T$ where E is evaporation and T is transpiration.**

6

7 **Reaction:**

8 As suggested by Savenije (2004) and based on the definition of total evaporation provided by
9 Shuttleworth (1993), we call the sum of interception (E_i), soil evaporation (E_s), transpiration (E_t),
10 and evaporation from water bodies (E_o) as “evaporation” (E). Thus, we did not apply the term of
11 “evapotranspiration” (ET), because we agree that they “are very different in terms of time scale,
12 time of occurrence, physical characteristics, climatic feedback and isotope composition” as
13 explained in Savenije (2004).

14

15 **Comment 2:**

16 **Page 3 Line 21: Does E_t have the same definition as the E_s defined in Line 16?**

17

18 **Reaction:**

19 Yes, as mentioned in reaction to comment 1, E_t is transpiration which is evaporation from the
20 soil moisture connected to the root zone, because that's where the trees get their water from.

21

22 **Comment 3:**

23 **Page 4 Lines 28-30: why's accounting for n is rarely necessary? Maybe it is better to explain it**
24 **briefly here.**

25

26 **Reaction:**

27 Miralles et al. (2010) and Pearce and Rowe (1981) both mentioned that accounting for n is rarely
28 necessary. Pearce and Rowe (1981) mentioned that "In many climates, however, such
29 adjustments will not be necessary, or small enough that they can be neglected". In our
30 interpretation this is because the number or times the interception storage can be filled and
31 completely emptied is limited once we assume a drying time of ca. 4 hours, which is common.
32 For 12 hours of day light, it means that n can be maximal 3 times. However, the chance that you
33 have 4 storms every 4 hours, with a drying period of 4 hours, is rather small for most climates. We
34 added this explanation in the revised manuscript.

35

36 **Comment 4:**

37 **Page 5 Line 36: If the inter-annual variability of the $D_{t,m}$ has any impact on the results?**

1 **Reaction:**

2 We explained in the manuscript (page 5, line 36-38) that taking a constant value for $D_{t,m}$ can be
3 problematic in energy-constrained areas. For water-constrained areas this is not a problem,
4 because there $E_{t,m}$ is determined by the LHS of the min-function ($A + B(P_m - E_{i,m})$) as can be
5 seen in Equation 7. For energy-constrained areas our assumption can be problematic. However,
6 in those areas often temperature and radiation follow a sinusoidal pattern without complex
7 double seasonality as e.g., occurs in the ITCZ. This implies that the overestimation of $E_{t,m}$ in
8 winter will be compensated (on the annual time scale) by the underestimation in summer time.
9 In addition, Gerrits et al. (2009) provided a sensitivity analysis on the effect of different $D_{t,m}$ on
10 total evaporation. Their results showed that total evaporation is sensitive to $D_{t,m}$ only once the
11 annual rainfall exceed ± 1000 mm/y. However, a sensitivity analysis conducted for clarifying this
12 issue for some parameters and variables (Figure 10 in the revised manuscript).

13
14 **Comment 5:**

15 **Page 5 Lines 37-37: “But in those relatively wet areas transpiration is underestimated in summer,**
16 **but overestimated in winter, which will cancel out on the annual scale.” Delete the first “But”?**

17
18 **Reaction:**

19 Thanks, it was done in the revised manuscript.

20
21 **Comment 6:**

22 **Page 7 Line 32: year-1**

23
24 **Reaction:**

25 Thanks, it was corrected in the revised manuscript.

26
27 **Comment 7:**

28 **Page 8 Lines 2-3: Is there any analysis in this study to demonstrate that the precipitation is the**
29 **major factor that caused the different results from different models?**

30
31 **Reaction:**

32 By providing a sensitivity analysis in the revised manuscript, we showed how the model is
33 sensitive to number of rain days and rain months. Moreover, the results of sensitivity analysis
34 conducted by Gerrits et al. (2009) shows that the results are significantly sensitive to change in
35 $n_{r,d}$. We revised the manuscript as follows:

36 “Different precipitation products applied in the models are likely the reason for the differences. As
37 found by Gerrits et al. (2009), the sensitivity of the model to the number of rain days and rain
38 months especially for the higher rates of precipitation can be a probable reason for poor

1 performance of a model especially for the forests with the highest amount of precipitation. In
2 Section “Sensitivity analysis” we will elaborate on the sensitivity of these parameters on the global
3 scale.”

4
5 **Comment 8:**

6 **Page 9 Lines 27-32: The global transpiration ratio estimated by Gerrits’ model is larger than nearly**
7 **all of the other studies listed, is there any reason?**

8
9 **Reaction:**

10 Our transpiration ratio estimate is indeed in the higher range compared to other models/studies,
11 however, the transpiration ratio estimated by Miralles et al. (2011) is higher than our model
12 (80% in comparison to 71%). Moreover, our estimation is close to that of Sutanto (2015) (69%)
13 and Good et al. (2015) (65%). Coenders-Gerrits et al. (2014) also found that based on the model
14 of Jasechko et al. (2013) transpiration ratio changes between 35% and 80%, which is in line with
15 our current findings. We added this information in the revised manuscript.

16
17 **Comment 9:**

18 **Page 10 Lines 27-29: Since the constant value of 0.935 mm in Equation 10 could be underestimated**
19 **for the forest floor interception, then what value is advised for the forest floor?**

20
21 **Reaction:**

22 Forest floor evaporation can be modeled for each region based on its characteristics (e.g., Wang-
23 Erlandsson et al. (2014)). Or typical values on S_{max} for the forest floor can be found in Table 22.1
24 of Gerrits and Savenije (2011). For example, in the UK for Pine (*Pinus sylvestris*), it is 0.6-1.7
25 mm (Walsh and Voigt, 1977), in Australia for Eucalyptus, it is 1.7 mm (Putuhena and Cordery,
26 1996) and in Luxembourg for Beech (*Fagus sylvatica*), it is 1-2.8 mm (Gerrits et al., 2010).

27
28 **References**

- 29 Coenders-Gerrits A M J, van der Ent R J, Bogaard T A, Wang-Erlandson L, Hrachowitz M and
30 Savenije H H G (2014) Uncertainties in transpiration estimates. *Nature* 506: E1–E2
31 Retrieved from <http://dx.doi.org/10.1038/nature12925>
- 32 Gerrits A M J, Pfister L and Savenije H H G (2010) Spatial and temporal variability of canopy
33 and forest floor interception in a beech forest. *Hydrological Processes* 24(21): 3011–3025
- 34 Gerrits A M J and Savenije H H G (2011) Forest Floor Interception. In D. F. Levia, D. E.
35 Carlyle-Moses & T. Tanaka (eds.), *Forest Hydrology and Biogeochemistry: Synthesis of*
36 *Past Research and Future Directions* (Vol. 216). Ecological Studies Series, No. 216,
37 Springer-Verlag, Heidelberg, Germany Retrieved from
38 <http://link.springer.com/10.1007/978-94-007-1363-5>

- 1 Gerrits A M J, Savenije H H G, Veling E J M and Pfister L (2009) Analytical derivation of the
2 Budyko curve based on rainfall characteristics and a simple evaporation model. *Water*
3 *Resources Research* 45: W04403 Retrieved from
4 <http://doi.wiley.com/10.1029/2008WR007308>
- 5 Good S P, Noone D and Bowen G (2015) Hydrologic connectivity constrains partitioning of
6 global terrestrial water fluxes. *Science* 349(6244): 175–177
- 7 Jasechko S, Sharp Z D, Gibson J J, Birks S J, Yi Y and Fawcett P J (2013) Terrestrial water
8 fluxes dominated by transpiration. *Nature* 496(7445): 347–350
- 9 Miralles D G, De Jeu R A M, Gash J H, Holmes T R H and Dolman A J (2011) Magnitude and
10 variability of land evaporation and its components at the global scale. *Hydrology and Earth*
11 *System Sciences* 15: 967–981
- 12 Miralles D G, Gash J H, Holmes T R H, De Jeu R A M and Dolman A J (2010) Global canopy
13 interception from satellite observations. *Journal of Geophysical Research Atmospheres*
14 115(16): 1–8
- 15 Pearce A J and Rowe L K (1981) Rainfall interception in a multi-storied, evergreen mixed
16 forest: estimates using Gash’s analytical model. *Journal of Hydrology* 49: 341–353
- 17 Putuhena W M and Cordery I (1996) Estimation of interception capacity of the forest floor.
18 *Journal of Hydrology* 180(1–4): 283–299 Retrieved from
19 <https://linkinghub.elsevier.com/retrieve/pii/0022169495028838>
- 20 Savenije H H G (2004) The importance of interception and why we should delete the term
21 evapotranspiration from our vocabulary. *Hydrological Processes* 18(8): 1507–1511
- 22 Shuttleworth W J (1993) Evaporation. In *Handbook of Hydrology*. McGraw-Hill, New York,
- 23 Sutanto S J (2015) Global transpiration fraction derived from water isotopologue datasets.
24 *Jurnal Teknik Hidraulik* 6(2): 131–146
- 25 Walsh R P D and Voigt P J (1977) Vegetation Litter: An Underestimated Variable in Hydrology
26 and Geomorphology. *Journal of Biogeography* 4(3): 253 Retrieved from
27 <https://www.jstor.org/stable/3038060?origin=crossref>
- 28 Wang-Erlandsson L, Van Der Ent R J, Gordon L J and Savenije H H G (2014) Contrasting roles
29 of interception and transpiration in the hydrological cycle - Part 1: Temporal characteristics
30 over land. *Earth System Dynamics* 5(2): 441–469

31

32

A global Budyko model to partition evaporation into interception and transpiration

Ameneh Mianabadi^{1,2}, Miriam Coenders–Gerrits^{2*}, Pooya Shirazi¹, Bijan Ghahraman¹, Amin Alizadeh¹

1- Ferdowsi University of Mashhad, Mashhad, Iran
2- Delft University of Technology, Delft, The Netherlands

*Corresponding author

Abstract

Evaporation is a very important flux in the hydrological cycle and links the water and energy balance of a catchment. The Budyko framework is often used to provide a first order estimate of evaporation, since it is a simple model where only rainfall and potential evaporation is required as input. Many researchers have ~~tried to improved~~ the Budyko framework by including more physics and catchment characteristics into the original equation. ~~However, this often resulted in additional parameters, which are unknown or difficult to determine.~~ In this paper we present an improvement of the previously presented Gerrits' model ("Analytical derivation of the Budyko curve based on rainfall characteristics and a simple evaporation model" in Gerrits et al, 2009 WRR), whereby total evaporation is calculated on the basis of simple interception and transpiration thresholds in combination with measurable parameters like rainfall dynamics and storage availability from remotely sensed data sources. While Gerrits' model was previously investigated for 10 catchments with different climate conditions and some parameters were assumed to be constant, in this study we applied the model on the global scale and fed with remotely sensed input data. The output of the model has been compared to two complex land-surface models STEAM and GLEAM, as well as the database of Landflux-EVAL. Our results show that total evaporation estimated by Gerrits' model is in good agreement with Landflux-EVAL, STEAM and GLEAM. Results also show that Gerrits' model underestimates interception in comparison to STEAM and overestimates it in comparison to GLEAM, while for transpiration the opposite is found. Errors in interception can partly be explained by differences in the interception definition that successively introduce errors in the calculation of transpiration. ~~Relating Comparing~~ to the Budyko framework, the model showed a ~~good~~ reasonable performance for total evaporation estimation. Our results also found a unimodal distribution of $\frac{E_t}{P}$, indicating that both increasing and decreasing aridity will result in decline in the fraction of precipitation transpired by plants for growth and metabolism.

Keywords: Budyko curves, interception, transpiration, remote sensing, evaporation

1 Introduction

2 Budyko curves are used as a first order estimate of annual evaporation as a function of annual
3 precipitation and potential evaporation. If the available energy is sufficient to evaporate the
4 available moisture, annual evaporation can approach annual precipitation (water-limited
5 situation). If the available energy is not sufficient, annual evaporation can approach potential
6 evaporation (energy-limited situation). Using the water balance and the energy balance and by
7 applying the definition of the aridity index and Bowen ratio, the Budyko framework can be
8 described as (Arora, 2002):

$$\frac{E_a}{P_a} = \frac{\phi}{1+f(\phi)} = F(\phi) \quad (1)$$

9 with E_a annual evaporation [L/T], P_a annual precipitation [L/T], $\frac{E_a}{P_a}$ the evaporation ratio [-], and
10 ϕ the aridity index which is defined as the potential evaporation divided by annual precipitation [-].
11 ~~Equation 1 is the base of a~~ All Budyko curves, which are developed by different researchers
12 (Table 1), have a similar pattern as equation 1.

13 The equations shown in Table 1 assume that the evaporation ratio is determined by climate only
14 and do not take into account the effect of other controls on the water balance. Therefore, some
15 researchers incorporated more physics into the Budyko framework. For example Milly (1994,
16 1993) investigated the root zone storage as an important secondary control on the water balance.
17 Choudhury (1999) used net radiation and a calibration factor in Budyko curves. Zhang et al. (2004,
18 2001) tried to add a plant-available water coefficient, Porporato et al. (2004) took into account the
19 maximum storage capacity, Yang et al. (2006, 2008) incorporated a catchment parameter, and
20 Donohue et al. (2007) tried to consider vegetation dynamics. Although ~~the incorporation of these~~
21 ~~additional processes improved the model performance, the main difficulty with these approaches~~
22 ~~is the determination of the parameter values. In practice, they are therefore often used as calibration~~
23 ~~parameters. The model of~~ Gerrits et al. (2009) aimed to develop an analytical model (hereafter
24 Gerrits' model) that is physically based and only uses measurable parameters, some of the required
25 input values are not available at the global scale. For example, carry over parameter (A),
26 interception storage capacity (S_{max}), and plant available water ($S_{u,max}$), were available for the 10
27 case study locations in Gerrits et al. (2009), but at the global scale such data was not available.
28 They tested the model output (i.e., interception evaporation, transpiration, and total evaporation)
29 on a couple of locations in the world, where the parameters could be determined, but not at the
30 global scale due to data limitations. However, Now with the current developments in remotely
31 sensed data, new opportunities have arisen to overcome this data limitation. In this study we aim
32 to find relations between the missing input parameters and remotely sensed data products, so the
33 Gerrits' model can be tested at the global scale.

34 One of those input parameters is the soil moisture storage. Recently, many studies (e.g., Chen et
35 al., 2013; Donohue et al., 2010; Istanbuloglu et al., 2012; Milly and Dunne, 2002; Wang, 2012;
36 Zhang et al., 2008) found that soil moisture storage change is a critical component in modelling
37 the interannual water balance. Including soil water information into the Budyko framework was
38 often difficult, because this information is not widely available. However, Gao et al. (2014)

1 presented a new method where the available soil water (which is often linked to soil water
 2 capacity) is derived from time series of rainfall and potential evaporation, plus a long-term runoff
 3 coefficient. These input time series ~~This data~~ can be ~~obtained~~derived locally (e.g., de Boer-Euser
 4 et al. (2016)), but can also be derived from remotely sensed data as shown by Wang-Erlandsson
 5 et al. (2016), which allows us to apply the method at the global scale and incorporate it in the
 6 Gerrits' model.

~~7 While Gerrits' model was only tested for 10 locations with different climatic conditions, the aim~~
 8 ~~of this study is to test Gerrits' model at the global scale. We used remotely sensed data to estimate~~
 9 ~~parameters, which were considered constant in Gerrits' model. These parameters are the maximum~~
 10 ~~soil moisture storage by the method of Gao et al (2014) and the~~ Next to using the method of Gao
 11 et al (2014) to globally estimate the maximum soil water storage ($S_{u,max}$), we also tested a method
 12 to derive the interception storage capacity (S_{max}) from remotely sensed data. These two
 13 parameters are required to make a first order estimate of total evaporation, and to partition this into
 14 interception evaporation and transpiration as well. The outcome is compared to more complex
 15 land-surface-atmosphere models ~~as well as to the Budyko curves of Table 1. Furthermore, the~~
 16 results of the model will be related to the Budyko framework for a better understanding of the
 17 partitioning of evaporation into transpiration and interception.

18 Methodology

19 Total evaporation (E) may be partitioned as follows (Shuttleworth, 1993):

$$E = E_i + E_t + E_o + E_s \quad (2)$$

20 in which E_i is interception evaporation, E_t is transpiration, E_o is evaporation from water bodies
 21 and E_s is evaporation from the soil, all with dimensions [LT^{-1}]. In this definition, interception is
 22 the amount of evaporation from any wet surface including canopy, understory, forest floor, and
 23 the top layer of the soil. Soil evaporation is defined as evaporation of the moisture in the soil that
 24 is connected to the root zone (de Groen and Savenije, 2006) and therefore is different from
 25 evaporation of the top layer of the soil (several millimeters of soil depth, which is here considered
 26 as part of the interception evaporation). Hence interception evaporation is the fast feedback of
 27 moisture to the atmosphere within a day from the rainfall event and soil evaporation is evaporation
 28 from the non-superficial soil constrained by soil moisture storage in the root zone. Like Gerrits et
 29 al. (2009), we assume that evaporation from soil moisture is negligible (or can be combined with
 30 interception evaporation). Evaporation from water bodies is used for inland open water, where
 31 interception evaporation and transpiration is zero. As a result, Equation 2 becomes:

$$E = E_o \quad \text{for water bodies} \quad (3a)$$

$$E = E_i + E_t \quad \text{for land surface} \quad (3b)$$

32 where E_i is direct feedback from short term moisture storage on vegetation, ground, and top layer,
 33 and E_t is evaporation from soil moisture storage in the root zone.

34 For modelling evaporation, it is important to consider that interception and transpiration have
 35 different time scales (i.e. the stock divided by the evaporative flux) (Blyth and Harding, 2011).

1 With a stock of a few millimetres and the evaporative flux of a few millimetres per day,
2 interception has a time scale in the order of one day (Dolman and Gregory, 1992; Gerrits et al.,
3 2009, 2007; Savenije, 2004; Scott et al., 1995). In the case of transpiration, the stock amounts to
4 tens to hundreds of millimetres and the evaporative flux to a few millimetres per day (Baird and
5 Wilby, 1999), resulting in a time scale in the order of month(s) (Gerrits et al., 2009). In Gerrits’
6 model it is successively assumed that interception and transpiration can be modelled as threshold
7 processes at the daily and monthly time scale, respectively. Rainfall characteristics are
8 successively used to temporally upscale from daily to monthly, and from monthly to annual. A full
9 description of the derivation and assumptions can be found in Gerrits et al. (2009). Here, we only
10 summarize the relevant equations (Table 2) and not the complete derivation. Since we now test
11 the model at the global scale, we do show how we estimated the required model parameters and
12 the inputs used.

13 **Interception**

14 Gerrits’ model considers evaporation from interception as a threshold process at daily time scale
15 (Equation 4, Table 2). Daily interception ($E_{i,d}$), then, is upscaled to monthly interception ($E_{i,m}$,
16 Equation 5, Table 2) by considering the frequency distribution of rainfall on a rain day (β -
17 parameter) and subsequently to annual interception ($E_{i,a}$, Equation 6, Table 2) by considering the
18 frequency distribution of rainfall in a rain month (κ_m -parameter) (see de Groen and Savenije
19 (2006), Gerrits et al. (2009)). A rain day is defined as a day with more than 0.1 mm day⁻¹ of rain
20 and a rain month is a month with more than 2 mm month⁻¹ of rain.

21 While Gerrits et al. (2009) assumed a constant interception threshold ($D_{i,d} = 5$ mm day⁻¹) for the
22 studied locations, we here use a globally variable value based on remote sensing data. The
23 interception threshold ($D_{i,d}$) is a daily average during the year yearly average and is either limited
24 by the daily interception storage capacity S_{max} (mm day⁻¹) or by the daily potential evaporation
25 (Equation 9, Table 2) and thus not seasonally variable. We can assume this, because for most
26 locations S_{max} is smaller than $E_{p,d}$ even if we consider a daily varying potential evaporation.
27 Additionally, S_{max} (based on LAI) could also be changed seasonally, however many studies show
28 that the storage capacity is not changing significantly between the leafed and leafless period (e.g.,
29 Leyton et al., 1967; Dolman, 1987; Rutter et al., 1975). Especially, once interception is defined in
30 a broad sense that it includes all evaporation from the canopy, understory, forest floor, and the top
31 layer of the soil: leaves that are dropped from the canopy remain their interception capacity as they
32 are on the forest floor in the leafless period. Furthermore, Gerrits et al (2010) showed with a Rutter-
33 like model that interception is more influenced by the rainfall pattern than by the storage capacity,
34 which was also found by Miralles et al. (2010). Hence, in interception modelling, the value of the
35 storage capacity is of minor concern, and seasonality is incorporated in the temporal rainfall
36 patterns.

37 The daily interception storage capacity should be seen as the maximum interception capacity
38 within one day, including the (partly) emptying and filling of the storage between events per day,
39 thus $S_{max} = n \cdot C_{max}$, where C_{max} [L] is the interception storage capacity of land cover. If there
40 is only one rain event per day ($n = 1$ day⁻¹) (Gerrits et al., 2010), S_{max} [LT⁻¹] equals C_{max} [L], as

1 is often found in literature. Despite proposing modifications for storms, which last more than one
2 day (Pearce and Rowe, 1981), and multiple storms per rain day (Mulder, 1985), ~~accounting for n~~
3 ~~is rarely necessary (Miralles et al., 2010).~~ Miralles et al. (2010) and Pearce and Rowe (1981) both
4 mentioned that accounting for n is rarely necessary. Pearce and Rowe (1981) mentioned that "In
5 many climates, however, such adjustments will not be necessary, or small enough that they can be
6 neglected". In our interpretation this is because the number of times the interception storage can
7 be filled and completely emptied is limited once we assume a drying time of a couple of hours
8 (e.g., 4), which is common (Wang-Erlandsson et al., 2014).

9 For $n = 1$, the interception storage capacity can be estimated from Von Hoyningen-Huene (1981),
10 which is obtained for a series of crops based on the leaf area index (LAI) (de Jong and Jetten,
11 2007) (Equation 10, Table 2). Since the storage capacity of the forest floor is not directly related
12 to LAI, it could be said that the 0.935 mm in Equation 10 is sort of the storage capacity of the
13 forest floor. Since this equation was developed for crops, it is likely that it underestimates
14 interception by forests with a denser understory and forest floor interception capacity.

15 Transpiration

16 Transpiration is considered as a threshold process at the monthly time scale ($E_{t,m}$ (mm month⁻¹),
17 Equation 7, Table 2) and successively is upscaled to annual transpiration ($E_{t,a}$ (mm year⁻¹),
18 Equation 8, Table 2) by considering the frequency distribution of the net monthly rainfall ($P_{n,m} =$
19 $P_m - E_{i,m}$) expressed with the parameter κ_n . To estimate the monthly and annual transpiration,
20 two parameters A and B are required. A is the initial soil moisture or carryover value (mm month⁻¹)
21 and B is dimensionless and described as Equation 15, where the dimensionless γ is obtained by
22 Equation 16.

23 Gerrits et al. (2009) assumed that the carry over value (A) is constant and used $A = 0, 5, 15, 20,$
24 mm month⁻¹, depending on the location, to determine annual transpiration. Also they considered
25 γ to be constant ($\gamma = 0.5$). In the current study, we determined these two parameters based on the
26 maximum root zone storage capacity ($S_{u,max}$). In equation 17, $\Delta t_m = 1$ month and S_b can be
27 assumed to be ~~50% to 80% of $S_{u,max}$~~ estimated by $aS_{u,max}$ (equation 18 in table 2), where a is
28 0.5-0.8 (de Groen, 2002; Shuttleworth, 1993). In this study we assumed ~~S_b~~ a to be ~~50% of $S_{u,max}$~~
29 0.5 as this value is commonly used for many crops (Allen et al., 1998). Furthermore, we assumed
30 that the monthly carry over A can be estimated as ~~$bS_{u,max}$~~ by equation 8 and in this study we
31 assumed $b = 0.2$ which gave the best global results for all land classes. In the sensitivity analysis
32 both the sensitivity of a and b towards total evaporation will be investigated. To estimate A and
33 γ , it is important to have a reliable database of $S_{u,max}$. For this purpose, we used the global
34 estimation of $S_{u,max}$ from Wang-Erlandsson et al. (2016) ~~(Fig. 1d)~~. $S_{u,max}$ is derived by the mass
35 balance method using satellite based precipitation and evaporation (Wang-Erlandsson et al., 2016).
36 Wang-Erlandsson et al. (2016) estimated the root zone storage capacity from the maximum soil
37 moisture deficit, as the integral of the outgoing flux (i.e. evaporation which is sum of transpiration,
38 evaporation, interception, soil moisture evaporation and open water evaporation) minus the
39 incoming flux (i.e. precipitation and irrigation). In their study, the root zone storage capacity was
40 defined as the total amount of water that plants can store to survive droughts. Note that this recent

1 method (Gao et al., 2014) to estimate $S_{u,max}$ does not require soil information, but only uses
2 climatic data. It is assumed that ecosystems adjust their storage capacity to climatic demands
3 irrespective of the soil properties. Under wet conditions Gao's method appeared to perform better.
4 For (semi-)arid climates the difference between this method and soil-based methods appear to be
5 small (de Boer-Euser et al., 2016).

6 Furthermore, Gerrits et al. (2009) estimated the average monthly transpiration threshold ($D_{t,m}$) as
7 $\frac{E_p - E_{t,a}}{n_a}$ (where n_a = number of months per year), which assumes that if there is little interception,
8 plants can transpire at the same rate as a well-watered reference grass as calculated with the
9 Penman-Monteith equation (University of East Anglia Climatic Research Unit, 2014). In reality,
10 most plants encounter more resistance (crop resistance) than grass, hence we used Equation 17,
11 Table 2 (Fredlund et al., 2012) to convert potential evaporation of reference grass (E_p) to potential
12 transpiration of a certain crop depending on LAI (i.e. the transpiration threshold $D_{t,m}$ [mm month⁻¹]).
13 Furthermore, similar to the daily interception threshold, we took a constant $D_{t,m}$, which can be
14 problematic in energy-constrained areas. ~~But in those relatively wet areas transpiration is~~
15 ~~underestimated in summer, but overestimated in winter, which will cancel out on the annual scale.~~
16 However, in those areas often temperature and radiation follow a sinusoidal pattern without
17 complex double seasonality as e.g., occurs in the ITCZ. This implies that the overestimation of
18 $E_{t,m}$ in winter will be compensated (on the annual time scale) by the underestimation in summer
19 time. By means of a sensitivity analysis the effect of a constant $D_{t,m}$ will be investigated.

20 Data

21 For precipitation we used the AgMERRA product from AgMIP climate forcing dataset (Ruane et
22 al., 2015), which has a daily time scale and a spatial resolution of 0.25°×0.25° (see Fig. 1a). The
23 spatial coverage of AgMERRA is globally for the years 1980-2010. The AgMERRA product is
24 available on the NASA Goddard Institute for Space Studies website
25 (<http://data.giss.nasa.gov/impacts/agmipcf/agmerra/>).

26 Potential evaporation (see Fig. 1b) data (calculated by FAO-Penman–Monteith equation (Allen et
27 al., 1998)) were taken from Center for Environmental Data Archival website
28 (<http://catalogue.ceda.ac.uk/uuid/4a6d071383976a5fb24b5b42e28cf28f>), produced by the
29 Climatic Research Unit (CRU) at the University of East Anglia (University of East Anglia Climatic
30 Research Unit, 2014). These data are at the monthly time scale over the period 1901-2013, and
31 has a spatial resolution of 0.5°×0.5°. We used the data of 1980-2010 in consistent with
32 precipitation dataset.

33 LAI data (Fig. 1c) were obtained from Vegetation Remote Sensing & Climate Research
34 (<http://sites.bu.edu/cliveg/datacodes/>) (Zhu et al., 2013). The spatial resolution of the data sets is
35 1/12 degree, with 15-day composites (2 per month) for the period July 1981 to December 2011.

36 The data of $S_{u,max}$ (Fig. 1d) is prepared data by Wang-Erlandsson et al. (2016) and is based on the
37 satellite based precipitation and evaporation with 0.5°×0.5° resolution over the period 2003-2013.
38 They used the USGS Climate Hazards Group InfraRed Precipitation with Stations (CHIRPS)

1 precipitation data at 0.05° (Funk et al., 2014) and the ensemble mean of three datasets of
 2 evaporation including CSIRO MODIS Reflectance Scaling EvapoTranspiration (CMRSET) at
 3 0.05° (Guerschman et al., 2009), the Operational Simplified Surface Energy Balance (SSEBop) at
 4 30" (Senay et al., 2013) and MODIS evapotranspiration (MOD16) at 0.05° (Mu et al., 2011). They
 5 calculated potential evaporation using Penman-Monteith equation (Monteith, 1965).

6 Model comparison and evaluation

7 The model performance was evaluated by comparing our results at the global scale to global
 8 evaporation estimates from other studies. Most available products only provide total evaporation
 9 estimates and do not distinguish between interception and transpiration. Therefore, we chose to
 10 compare our interception and transpiration results to two land surface models: The Global Land
 11 Evaporation Amsterdam Model (GLEAM) (v3.0a) database (Martens et al., 2017; Miralles et al.,
 12 2011a) and Simple Terrestrial Evaporation to Atmosphere Model (STEAM) (Wang-Erlandsson et
 13 al., 2014, Wang-Erlandsson et al., 2016). GLEAM estimates different fluxes of evaporation
 14 including transpiration, interception, bare soil evaporation, snow sublimation and open water
 15 evaporation. STEAM, on the other hand, estimates the different components of evaporation
 16 including transpiration, vegetation interception, floor interception, soil moisture evaporation, and
 17 open water evaporation. Thus for the comparison of interception we used the sum of canopy and
 18 floor interception and soil evaporation from STEAM and canopy interception and bare soil
 19 evaporation from GLEAM. Furthermore, STEAM includes an irrigation module (Wang-
 20 Erlandsson et al., 2014), while Miralles et al. (2011) mentioned that they did not include irrigation
 21 in GLEAM, but the assimilation of the soil moisture from satellite would account for it as soil
 22 moisture adjusted to seasonal dynamics of any region. The total evaporation was also compared
 23 to LandFlux-EVAL products (Mueller et al., 2013). GLEAM database (www.gleam.eu) is
 24 available for 1980-2014 with a resolution of 0.25°×0.25° and STEAM model was performed for
 25 2003-2013 with a resolution of 1.5°×1.5°. LandFlux-EVAL data
 26 (<https://data.iac.ethz.ch/landflux/>) is available for 1989-2005. We compared Gerrits' model to
 27 other products based on the land cover to judge the performance of the model for different types
 28 of land cover. The global land cover map (Channan et al., 2014; Friedl et al., 2010) was obtained
 29 from <http://glcf.umd.edu/data/lc/>. ~~Lastly, we also compared our results to the Budyko curves of~~
 30 ~~Schreiber, O'Idokop, Pike and Budyko (Table 1).~~ We used root mean square error (RMSE) (Eq.
 31 20), mean bias error (MBE) (Eq. 21) and relative error (RE) (Eq. 22) to evaluate the results.

$$\text{RMSE} = \sqrt{\frac{\sum_{i=1}^n (x_{iG} - x_{iM})^2}{n}} \quad (20)$$

$$\text{MBE} = \frac{\sum_{i=1}^n (x_{iG} - x_{iM})}{n} \quad (21)$$

$$\text{RE} = \frac{\bar{x}_G - \bar{x}_M}{\bar{x}_G} \times 100 \quad (22)$$

32 In these equations, x_{iM} is evaporation of the benchmark models to which Gerrits' model is
 33 compared for pixel i , x_{iG} is evaporation from Gerrits' model for pixel i , \bar{x}_G is the average
 34 evaporation of Gerrits' model, \bar{x}_M is the average evaporation of the benchmark models and n is

1 the number of pixels of the evaporation map. Negative MBE and RE show the Gerrits' model
2 underestimates evaporation and vice versa. As the spatial resolution of the products is different,
3 we regridded all the products to the coarsest resolution ($1.5^{\circ} \times 1.5^{\circ}$) for the comparison.
4 Furthermore, the comparisons were shown for each land cover using the Taylor diagram (Taylor,
5 2001). ~~This A Taylor~~ diagram can provide a concise statistical summary of how the models are
6 comparable to the reference data (observation or given model) in terms of their correlation, RMSE,
7 and the ratio of their variances. In this paper, the reference data is Gerrits' model. Since the
8 different models for different land cover types have been used in this study, which have different
9 numerical values, the results are normalized by the reference data. It should be noted that the
10 standard deviation of the reference data is normalized by itself and, therefore, it is plotted at unit
11 distance from the origin along the horizontal axis (Taylor, 2001). According to the Taylor diagram,
12 when the points are close to reference data ('Ref' in Figures [2](#), [4](#) and [6](#)~~3~~, [5](#), [7](#) and [9](#)), it shows that
13 the RMSE is less and the correlation is higher and therefore, the models are in a more reasonable
14 agreement.

15 Results and discussion

16 Total evaporation comparison

17 Figure [12](#) shows the mean annual evaporation from Gerrits' model, Landflux-EVAL, STEAM and
18 GLEAM data sets. In general, the spatial distribution of evaporation simulated by Gerrits' model
19 is similar to that of the benchmark models. Figure [2a-1a](#) demonstrates that, as expected, the highest
20 annual evaporation, which is the sum of interception evaporation and transpiration, occurs in
21 tropical evergreen broadleaf forests and the lowest rate occurs in the barren and sparsely vegetated
22 desert regions. Total evaporation varies between almost zero in arid regions to more than 1500
23 mm year⁻¹ in the tropics.

24 As can be seen in Figure [12](#) there exist also large differences between STEAM, GLEAM and
25 Landflux-EVAL. ~~Different products of precipitation (and other global data bases) applied for the
26 models is likely the reason. For example, the sensitivity of the model to the number of rain days
27 and rain months especially for the higher rate of precipitation (Gerrits et al., 2009) can be a
28 probable reason for poor performance of a model especially for evergreen forests with the highest
29 amount of precipitation. Different precipitation products used in the models are likely the reason
30 for the differences. As found by Gerrits et al. (2009), the sensitivity of the model to the number of
31 rain days and rain months especially for the higher rates of precipitation can be a probable reason
32 for poor performance of a model especially for the forests with the highest amount of precipitation.
33 In Section "Sensitivity analysis" we will elaborate on the sensitivity of these parameters on the
34 global scale.~~

35 Mean annual evaporation contributions per land cover type from Gerrits' model and other products
36 as well as RMSE, MBE and RE are shown in Table 3. Globally, mean annual evaporation
37 estimated (for the overlapped pixels with $1.5^{\circ} \times 1.5^{\circ}$ resolution) by Gerrits' model, Landflux-
38 EVAL, STEAM and GLEAM are 443, 469, 475 and 462 mm year⁻¹, respectively. Our results are
39 comparable to those of Haddeland et al. (2011), where the simulated global terrestrial evaporation
40 ranges between 415 and 586 mm year⁻¹ for the period 1985–1999. Generally, Gerrits' model

1 overestimates evaporation for most land cover types in comparison to Landflux-EVAL and
2 GLEAM, and underestimates in comparison to STEAM (see also MBE and RE). Since the number
3 of pixels covered by each land use is different, RMSE, MBE and RE cannot be comparable
4 between land cover types. RMSE, MBE and RE for each land cover type show that, generally,
5 Gerrits' model is in a better agreement with Landflux and GLEAM than STEAM. The Taylor
6 diagram for total evaporation estimated by Gerrits' model in comparison to Landflux-EVAL,
7 STEAM and GLEAM for all data (No. 1 in Fig. 32) and for each land cover type (No.2 to No.11
8 in Fig. 32) also indicates that Gerrits' model has a better agreement with Landflux-EVAL and
9 GLEAM than STEAM model, especially for evergreen broadleaf forest, shrublands, savannas and
10 croplands (see also Table 3).

11 Annual interception comparison

12 While Wang-Erlandsson et al. (2014; 2016) estimated canopy interception, floor interception and
13 soil evaporation separately, in the current study we assumed that these three components of
14 evaporation can be lumped as interception evaporation. Figure 4-3 shows the mean annual
15 evaporation from interception at the global scale estimated by Gerrits' model, STEAM and
16 GLEAM. In this figure, interception from STEAM is calculated by the sum of canopy interception,
17 floor interception and soil evaporation. Furthermore, interception from GLEAM is calculated as
18 the sum of canopy interception and bare soil evaporation (GLEAM does not estimate floor
19 interception). In general, the spatial distribution of Gerrits' simulated interception is partly similar
20 to that of STEAM and GLEAM. In the tropics, with high amounts of annual precipitation and high
21 storage capacity due to the dense vegetation (evergreen broadleaf forests and savannas), annual
22 interception shows the highest values. Table 4 shows the average of interception, RMSE, MBE
23 and RE per land cover type. This table indicates that Gerrits' model underestimates interception
24 in comparison to STEAM for all land cover types. Table 4 also shows that, in comparison to
25 GLEAM, Gerrits' model overestimates interception for all land cover types, because in GLEAM
26 floor interception has not been taken into account. Figure 5-4 also shows that Gerrits' model is in
27 better agreement with STEAM (especially for grasslands and mixed forest) than GLEAM. The
28 reason for an underestimated interception in comparison to STEAM could be the role of the
29 understory. LAI does not account for understory, therefore maybe S_{max} should be larger than
30 modeled with Equation 10. However, there is almost no data available to estimate the interception
31 storage capacity of the forest floor at the global scale.

~~32 We also compared our interception ratio E_i/E (Fig. 10) with some studies that looked after
33 evaporation partitioning. Wang-Erlandsson defined interception in a slightly different way, hence
34 we compared our calculated E_i/E with the sum of soil moisture evaporation ratio, vegetation
35 interception ratio and floor interception ratio which are presented in Fig. 5.b, 5.c and 5.d in Wang-
36 Erlandsson et al. (2014), respectively. While the results of Wang-Erlandsson et al. (2014) showed
37 that vegetation interception in arid regions with no vegetation cover is zero, soil moisture and floor
38 interception show a considerable percentage of total evaporation. Our results also show that $\frac{E_i}{E}$ in
39 arid regions is close to 100%. Therefore, the interception ratio in this study is in a reasonable
40 agreement with the results of Wang-Erlandsson et al. (2014). It is also comparable to the sum of
41 bare soil evaporation and canopy interception from GLEAM (Martens et al., 2017).~~

1 Annual transpiration comparison

2 Figure 6-5 illustrates the mean annual transpiration estimated by Gerrits' model, STEAM and
3 GLEAM. The spatial distribution is similar to the results of STEAM and GLEAM. Mean annual
4 transpiration varies between zero mm year⁻¹ for arid areas in the north of Africa (Sahara) to more
5 than 1000 mm year⁻¹ in the tropics in South America. The results show that the highest annual
6 transpiration occurs in evergreen broadleaf forests with the highest amount of precipitation and
7 dense vegetation (see also Table 5). Figure 6e-5c shows that GLEAM, in comparison to Gerrits'
8 model, overestimates the transpiration in some regions especially in the tropics in South America
9 and Central Africa. Figure 56b also shows that STEAM is different from Gerrits' model over some
10 regions like India, western China and North America as well as in the tropics. Table 5 (MBE and
11 RE) also indicates that Gerrits' model underestimates transpiration in comparison to GLEAM and
12 overestimates in comparison to STEAM. The Taylor diagram (Fig. 67) shows global annual
13 transpiration of Gerrits' model is closer to that of GLEAM than STEAM, representing that the
14 Gerrits' model is in a more reasonable agreement with GLEAM for transpiration estimation.

15 ~~Similar to the interception ratio, we also compared our transpiration ratio E_t/E (Fig 10), and found~~
16 ~~that the results are in a reasonable agreement with STEAM (See Fig. 5.a, Wang Erlandsson et al.~~
17 ~~(2014)) and GLEAM (See Fig. 9.e, Martens et al. (2017)). Moreover, Gglobal transpiration ratio~~
18 ~~estimated by Gerrits' model is 71% which is comparable to the ratio estimated by other studies~~
19 ~~(e.g. 80% (Miralles et al., 2011b), 69% (Sutanto, 2015), 65% (Good et al., 2015), 62% (Maxwell~~
20 ~~and Condon, 2016), 62% (Lian et al., 2018), 61% (Schlesinger and Jasechko, 2014), 57% (Wei et~~
21 ~~al., 2017), 52% (Choudhury and Digirolamo, 1998), 48% (Dirmeyer et al., 2006) and 41%~~
22 ~~(Lawrence et al., 2007). Additionally, Coenders-Gerrits et al. (2014) found that based on the model~~
23 ~~of Jasechko et al. (2013) transpiration ratio changes between 35% and 80%, which is in line with~~
24 ~~our current findings.~~

25 Analyzing the results through Budyko framework

26 ~~Figure 8 shows the mean annual evaporation derived from four non-parametric Budyko curves~~
27 ~~(Table 1) including Schreiber (1904), Ol'dekop (1911), Pike (1964) and Budyko (1974). The~~
28 ~~global mean annual evaporation estimated by Pike and Budyko are close (445 and 439 mm year~~
29 ~~⁻¹, respectively). Schreiber underestimates the mean annual evaporation in comparison to Ol'dekop,~~
30 ~~Pike and Budyko, especially in regions with a higher rate of evaporation. Table 6 shows the mean~~
31 ~~annual evaporation estimated by these four curves per land cover type in comparison to Gerrits'~~
32 ~~model as well as RMSE, MBE and RE. The results show that mean annual evaporation of Gerrits'~~
33 ~~model for forests is closer to that of Ol'dekop and for the other land classes it is closer to that of~~
34 ~~Budyko. Global mean annual evaporation is close to Pike where RE is almost zero. Taylor diagram~~
35 ~~(Fig. 9) shows that, in comparison to the Budyko curves, Gerrits' model performs well for all land~~
36 ~~cover types except for Evergreen broadleaf and Deciduous needleleaf forest. Evergreen broadleaf~~
37 ~~forest shows a significant overestimation of evaporation by Gerrits' model in comparison to~~
38 ~~Budyko curves. One of the reasons for these differences can be the used precipitation product as~~
39 ~~Gerrits et al. (2009) mentioned that the number of rain months per year, is the most sensitive~~
40 ~~parameter. Furthermore, as mentioned before in Section "Annual interception comparison", the~~

1 role of the understory, which has not been taken into account in S_{max} equation, can be a source of
2 error for the poor interception performance (and therefore total evaporation) in forests.

3 We evaluated the relation between evaporation fluxes and energy/water limitation in the Budyko
4 framework as provided by Miralles et al. (2016) and Good et al. (2017) to see how our model can
5 be related to the Budyko framework and how the energy and water limitations can be interpreted
6 by our model. Figure 7 shows the density plot of $\frac{E}{P}$ versus $\frac{E_p}{P}$ within the Budyko framework. For
7 calculating $\frac{E}{P}$ and $\frac{E_p}{P}$ for all models, precipitation and potential evaporation data are the same as
8 used in this study. This figure indicates that, while Gerrits' model does not perform well in
9 comparison to STEAM and GLEAM, it follows the framework in a reasonable manner.
10 Furthermore, the results are comparable to the results of Miralles et al. (2016) (see Fig. 11 in their
11 paper). The partition of evaporation related to the land cover within the Budyko framework is
12 presented in Figure 8. According to this figure, interception as estimated by Gerrits' model is
13 closer to that of GLEAM rather than STEAM, but transpiration is close to both models. For mean
14 annual total evaporation, Gerrits' model is more similar to GLEAM than STEAM for all land
15 covers except for grasslands and shrublands. Moreover, the distribution of $\frac{E_t}{P}$ is comparable to that
16 of Good et al. (2017) (Figure 1.a in their paper). Their results showed a unimodal $\frac{E_t}{P}$ distribution
17 indicating that both increasing and decreasing aridity will result in a decline in the fraction of
18 precipitation transpired by plants for growth and metabolism. This distribution is also seen in
19 Figure 9, where the plot is provided based on the average of $\frac{E}{P}$ for each aridity index ($\frac{E_p}{P}$). This
20 figure is also comparable to figure 1.c in Good et al. (2017)'s paper.

21 Sensitivity analysis

22 In our sensitivity analysis we investigated the sensitivity of the three parameters that are related to
23 transpiration (constants a and b , and threshold $D_{t,m}$), and the effect of the number of rain days and
24 rain months on the total evaporation calculation. All parameters were in- and decreased by 10%.
25 The analysis shows that the model is not too sensitive to parameter a , where a $\pm 10\%$ change in a
26 leads to a minor $\mp 0.4\%$ change in $\frac{E}{P}$ (See Fig. 10.a). Thus, the model is not sensitive to changes in
27 parameter a . Similar results were found for parameter b , where a $\pm 10\%$ change in b resulted only
28 in a $\pm 3.5\%$ change in $\frac{E}{P}$ (Fig. 10.b). Moreover, a $\pm 10\%$ change in both $n_{r,d}$ and $n_{r,m}$ leads to a ± 2.2
29 change in $\frac{E}{P}$ (Fig. 10.c and 10.d). The most sensitive parameter is $D_{t,m}$, where a $\pm 10\%$ change in
30 $D_{t,m}$ resulted in a $\pm 4\%$ change in $\frac{E}{P}$ (Fig. 10.e). In conclusion, $D_{t,m}$ and b are the most sensitive
31 parameters for the estimation of $\frac{E}{P}$; however, it seems that the sensitivity is not that much different
32 per land class, except for grasslands and shrublands, which may arise from the underestimation of
33 interception in Gerrits' model for short vegetation. This underestimation is obtained, because the
34 relation between S_{max} and LAI might not be valid for short vegetation. This also might be due to
35 the wide range of gridded points belong to grasslands and shrublands as shown by density plot of
36 $\frac{E}{P}$ versus $\frac{E_p}{P}$ in Figure 11.

1 Conclusion

2 In the current study we revised and applied a simple evaporation model proposed by Gerrits et al.
3 (2009) at the global scale. Instead of locally calibrated model parameters we now only used
4 parameters derived from remotely sensed data. Furthermore, we implemented in the Gerrits'
5 model a new definition of the root zone storage capacity from Gao et al (2014).

6 Comparing our results for total evaporation to Landflux-EVAL estimates show that Gerrits' model
7 is in good agreement with Landflux-EVAL. The highest mean annual evaporation rates are found
8 in evergreen broadleaf forests (1367 mm year⁻¹), deciduous broadleaf forests (796 mm year⁻¹) and
9 savannas (695 mm year⁻¹) and the lowest ones are found in shrublands (203 mm year⁻¹) and
10 grasslands (275 mm year⁻¹). Generally, Gerrits' model overestimates in comparison to Landflux-
11 EVAL and GLEAM, and underestimates in comparison to STEAM.

12 Gerrits' model underestimates interception in comparison to STEAM for all land covers. On the
13 other hand, the model overestimates interception in comparison to GLEAM, since GLEAM does
14 not include floor interception. Although we tried to correct for the different definitions of
15 interception, the results may be biased. The relatively worse performance in forests ecosystems
16 could be explained by the effect of understory. This is not taken into account in Gerrits' model,
17 while the understory can also intercept water. We could say that the constant value of 0.935 mm
18 in Equation 10 reflects the forest floor interception storage capacity, but since this number was
19 derived for crops, it is likely an underestimation. Therefore, better estimation of S_{max} to account
20 for forest floor interception is recommended.

21 Estimated transpiration by Gerrits' model is in reasonable agreement with GLEAM and STEAM.
22 Gerrits' model underestimates transpiration in comparison to GLEAM (RE=-4%) and
23 overestimates in comparison to STEAM (RE=+12%). The scatter plots showed that, in comparison
24 to GLEAM and STEAM, Gerrits' model performs well for all land cover types. Also the
25 transpiration ratio corresponded well in comparison to those of GLEAM and STEAM. The results
26 also showed that the global transpiration ratio estimated by Gerrits' model (71%) is approximately
27 comparable to the other studies.

28 ~~Comparing Gerrits' model to some Budyko curves, shows that the model performed well, but in~~
29 ~~areas with few number of rain months, evaporation is not close to the Budyko curves of Schreiber,~~
30 ~~Ol'dekop, Pike and Budyko. This is likely caused by the fact that Gerrits' model is rather sensitive~~
31 ~~to the number of rain days and rain months.~~

32 Our results are also related to the Budyko framework and we found similar to Good et al. (2017)
33 that the distribution of $\frac{E_t}{P}$ is unimodal, indicating that both increasing and decreasing aridity will
34 result in decline in the fraction of precipitation transpired by plants for growth and metabolism.

35 By comparing all products, we found that, in general, there are large differences between STEAM,
36 GLEAM and Landflux-EVAL. The most convincing reason for this discrepancy lies in the
37 different products for precipitation (and other global data sets), which have been used for the
38 different models. The Gerrits' model is sensitive to the number of rain days and months especially

1 for the higher rates of precipitation. Nonetheless, our sensitivity analysis of parameters a and b
2 and $n_{r,d}$, $n_{r,m}$ and $D_{t,m}$ shows that $D_{t,m}$ and b are the most sensitive parameters for the estimation
3 of $\frac{E}{p}$.

4 Generally, it should be mentioned that the underlying reasoning of the Gerrits' model is to
5 recognize the characteristic time scales of the different evaporation processes (i.e. interception
6 daily and transpiration monthly). In Gerrits et al. (2009) (and in the current paper as well), this has
7 been done by taking yearly averages for the interception ($D_{i,d}$, mm day⁻¹) and transpiration
8 threshold ($D_{t,m}$, mm month⁻¹) in combination with the temporal distribution functions for daily
9 and monthly (net) rainfall. Hence, the seasonality is incorporated in the temporal rainfall patterns,
10 and not in the evaporation thresholds. This is a limitation of the currently used approach and could
11 be the focus of a new study by investigating how seasonal fluctuating thresholds (based on LAI
12 and/or a simple cosine function) would affect the results. This could be a significant
13 methodological improvement of the Gerrits' model, but will have mathematical implications on
14 the analytical model derivation. It will improve the monthly evaporation estimates, but we expect
15 that the consequences at the annual time scale (which is the focus of the current paper) will be less
16 severe. The strength of the Gerrits' model is that, in comparison to other models, it is a very simple
17 and in spite of its simplicity, the Gerrits' model performs quite well.

18 **Acknowledgment**

19 This research was partly funded by NWO Earth and Life Sciences (ALW), veni-project
20 863.15.022, the Netherlands. Furthermore, we would like to thank Iran's Ministry of Science,
21 Research and Technology for supporting this research and the mobility fellowship. We also would
22 like to thank Jie Zhou, Lan Wang-Erlandsson, Kamran Davary, Shervan Gharari and Hubert
23 Savenije for their kind helps and comments.

24 **References**

- 25 Allen, R., Pereira, L., Raes, D., Smith, M., 1998. Crop evapotranspiration: Guidelines for
26 computing crop water requirements. FAO Irrig. Drain. Pap. 56. FAO, Rome, Italy, 300 p.
- 27 Arora, V.K., 2002. The use of the aridity index to assess climate change effect on annual runoff.
28 J. Hydrol. 265, 164–177. doi:10.1016/S0022-1694(02)00101-4
- 29 Baird, A.J., Wilby, R.L., 1999. Eco-hydrology: Plants and Water in Terrestrial and Aquatic
30 Environments. Routledge, London.
- 31 Blyth, E., Harding, R.J., 2011. Methods to separate observed global evapotranspiration into the
32 interception, transpiration and soil surface evaporation components. Hydrol. Process. 25,
33 4063–4068. doi:10.1002/hyp.8409
- 34 Budyko, M.I., 1974. Climate and life. Academic Press, Orlando, Fla.
- 35 Channan, S., Collins, K., Emanuel, W.R., 2014. Global mosaics of the standard MODIS land
36 cover type data. College Park, Maryland, USA.
- 37 Chen, X., Alimohammadi, N., Wang, D., 2013. Modeling interannual variability of seasonal

- 1 evaporation and storage change based on the extended Budyko framework. *Water Resour.*
2 *Res.* 49, 6067–6078. doi:10.1002/wrcr.20493
- 3 Choudhury, B., 1999. Evaluation of an empirical equation for annual evaporation using field
4 observations and results from a biophysical model. *J. Hydrol.* 216, 99–110.
5 doi:10.1016/S0022-1694(98)00293-5
- 6 Choudhury, B., Digirolamo, N.E., 1998. A biophysical process-based estimate of global land
7 surface evaporation using satellite and ancillary data I . Model description and comparison
8 with observations. *J. Hydrol.* 205, 164–185.
- 9 Coenders-Gerrits, A.M.J., van der Ent, R.J., Bogaard, T.A., Wang-Erlandson, L., Hrachowitz,
10 M., Savenije, H.H.G., 2014. Uncertainties in transpiration estimates. *Nature* 506, E1–E2.
11 doi:10.1038/nature12925
- 12 de Boer-Euser, T., McMillan, H.K., Hrachowitz, M., Winsemius, H.C., Savenije, H.H.G., 2016.
13 Influence of soil and climate on root zone storage capacity. *Water Resour. Res.* 17,
14 accepted. doi:10.1002/2015WR018115
- 15 de Groen, M.M., 2002. Modelling interception and transpiration at monthly time steps :
16 introducing daily variability through Markov chains.
- 17 de Groen, M.M., Savenije, H.H.G., 2006. A monthly interception equation based on the
18 statistical characteristics of daily rainfall. *Water Resour. Res.* 42, W12417.
19 doi:10.1029/2006WR005013
- 20 de Jong, S.M., Jetten, V.G., 2007. Estimating spatial patterns of rainfall interception from
21 remotely sensed vegetation indices and spectral mixture analysis. *Int. J. Geogr. Inf. Sci.* 21,
22 529–545. doi:10.1080/13658810601064884
- 23 Dirmeyer, P.A., Gao, X., Zha, M., Guo, Z., Oki, T., Hanasaki, N., 2006. GSWP-2: Multimodel
24 analysis and implications for our perception of the land surface. *Bull. Am. Meteorol. Soc.*
25 87, 1381–1397. doi:10.1175/BAMS-87-10-1381
- 26 Dolman, a J., Gregory, D., 1992. The Parametrization of Rainfall Interception In GCMs. *Q. J. R.*
27 *Meteorol. Soc.* 118, 455–467. doi:10.1002/qj.49712051713
- 28 Donohue, R.J., Roderick, M.L., McVicar, T.R., 2007. On the importance of including vegetation
29 dynamics in Budyko ’ s hydrological model. *Hydrol. Earth Syst. Sci.* 11, 983–995.
- 30 Donohue, R.J., Roderick, M.L., McVicar, T.R., 2010. Can dynamic vegetation information
31 improve the accuracy of Budyko’s hydrological model? *J. Hydrol.* 390, 23–34.
32 doi:10.1016/j.jhydrol.2010.06.025
- 33 Fredlund, D.G., Rahardjo, H., Fredlund, M.D., 2012. *Unsaturated Soil Mechanics in Engineering*
34 *Practice.* John Wiley & Sons, Ltd. doi:10.1002/9781118280492
- 35 Friedl, M.A., Sulla-Menashe, D., Tan, B., Schneider, A., Ramankutty, N., Sibley, A., Huang, X.,
36 2010. MODIS Collection 5 global land cover: Algorithm refinements and characterization
37 of new datasets, 2001-2012, Collection 5.1 IGBP Land Cover. Boston, MA, USA.
- 38 Gao, H., Hrachowitz, M., Schymanski, S.J., Fenicia, F., Sriwongsitanon, N., Savenije, H.H.G.,
39 2014. Climate controls how ecosystems size the root zone storage capacity at catchment
40 scale. *Geophys. Res. Lett.* 41, 7916–7923. doi:10.1002/2014GL061668

- 1 Gerrits, A.M.J., Pfister, L., Savenije, H.H.G., 2010. Spatial and temporal variability of canopy
2 and forest floor interception in a beech forest. *Hydrol. Process.* 24, 3011–3025.
3 doi:10.1002/hyp.7712
- 4 Gerrits, A.M.J., Savenije, H.H.G., Hoffmann, L., Pfister, L., 2007. New technique to measure
5 forest floor interception – an application in a beech forest in Luxembourg. *Hydrol. Earth
6 Syst. Sci.* 11, 695–701. doi:10.5194/hess-11-695-2007
- 7 Gerrits, A.M.J., Savenije, H.H.G., Veling, E.J.M., Pfister, L., 2009. Analytical derivation of the
8 Budyko curve based on rainfall characteristics and a simple evaporation model. *Water
9 Resour. Res.* 45, W04403. doi:10.1029/2008WR007308
- 10 Good, S.P., Moore, G.W., Miralles, D.G., 2017. A mesic maximum in biological water use
11 demarcates biome sensitivity to aridity shifts. *Nat. Ecol. Evol.* 1, 1883–1888.
12 doi:10.1038/s41559-017-0371-8
- 13 Good, S.P., Noone, D., Bowen, G., 2015. Hydrologic connectivity constrains partitioning of
14 global terrestrial water fluxes. *Science* (80-.). 349, 175–177.
- 15 Guerschman, J.P., Van Dijk, A.I.J.M., Mattersdorf, G., Beringer, J., Hutley, L.B., Leuning, R.,
16 Pipunic, R.C., Sherman, B.S., 2009. Scaling of potential evapotranspiration with MODIS
17 data reproduces flux observations and catchment water balance observations across
18 Australia. *J. Hydrol.* 369, 107–119. doi:10.1016/j.jhydrol.2009.02.013
- 19 Haddeland, I., Clark, D.B., Franssen, W., Ludwig, F., Voß, F., Arnell, N.W., Bertrand, N., Best,
20 M., Folwell, S., Gerten, D., Gomes, S., Gosling, S.N., Hagemann, S., Hanasaki, N.,
21 Harding, R., Heinke, J., Kabat, P., Koirala, S., Oki, T., Polcher, J., Stacke, T., Viterbo, P.,
22 Weedon, G.P., Yeh, P., 2011. Multimodel Estimate of the Global Terrestrial Water
23 Balance : Setup and First Results. *J. Hydrometeorol.* 12, 869–884.
24 doi:10.1175/2011JHM1324.1
- 25 Istanbuluoglu, E., Wang, T., Wright, O.M., Lenters, J.D., 2012. Interpretation of hydrologic
26 trends from a water balance perspective: The role of groundwater storage in the Budyko
27 hypothesis. *Water Resour. Res.* 48, W00H16. doi:10.1029/2010WR010100
- 28 Lawrence, D.M., Thornton, P.E., Oleson, K.W., Bonan, G.B., 2007. The Partitioning of
29 Evapotranspiration into Transpiration , Soil Evaporation , and Canopy Evaporation in a
30 GCM : Impacts on Land – Atmosphere Interaction. *J. Hydrometeorol.* 8, 862–880.
31 doi:10.1175/JHM596.1
- 32 Lian, X., Piao, S., Huntingford, C., Li, Y., Zeng, Z., Wang, X., Ciais, P., Mcvicar, T.R., Peng, S.,
33 Ottlé, C., Yang, H., Yang, Y., Zhang, Y., Wang, T., 2018. CMIP5 models constrained by
34 observations. *Nat. Clim. Chang.* 8, 640–646. doi:10.1038/s41558-018-0207-9
- 35 Martens, B., Miralles, D.G., Lievens, H., Van Der Schalie, R., De Jeu, R.A.M., Fernández-
36 Prieto, D., Beck, H.E., Dorigo, W.A., Verhoest, N.E.C., 2017. GLEAM v3 : satellite-based
37 land evaporation and root-zone soil moisture. *Geosci. Model Dev.* 10, 1903–1925.
38 doi:10.5194/gmd-10-1903-2017
- 39 Maxwell, R.M., Condon, L.E., 2016. Connections between groundwater flow and transpiration
40 partitioning. *Science* (80-.). 353, 377–380.
- 41 Milly, P.C.D., 1994. Climate, soil water storage, and the average annual water balance. *Water*

- 1 Resour. Res. 30, 2143–2156. doi:10.1029/94WR00586
- 2 Milly, P.C.D., 1993. An analytic solution of the stochastic storage problem applicable to soil
3 water. *Water Resour. Res.* 29, 3755–3758. doi:10.1029/93WR01934
- 4 Milly, P.C.D., Dunne, K. a., 2002. Macroscale water fluxes 2. Water and energy supply control
5 of their interannual variability. *Water Resour. Res.* 38, 24-1-24-9.
6 doi:10.1029/2001WR000760
- 7 Miralles, D.G., De Jeu, R.A.M., Gash, J.H., Holmes, T.R.H., Dolman, A.J., 2011. Magnitude and
8 variability of land evaporation and its components at the global scale. *Hydrol. Earth Syst.*
9 *Sci.* 15, 967–981. doi:10.5194/hess-15-967-2011
- 10 Miralles, D.G., Gash, J.H., Holmes, T.R.H., De Jeu, R.A.M., Dolman, A.J., 2010. Global canopy
11 interception from satellite observations. *J. Geophys. Res. Atmos.* 115, 1–8.
12 doi:10.1029/2009JD013530
- 13 Miralles, D.G., Holmes, T.R.H., De Jeu, R.A.M., Gash, J.H., Meesters, A.G.C.A., Dolman, A.J.,
14 2011. Global land-surface evaporation estimated from satellite-based observations. *Hydrol.*
15 *Earth Syst. Sci.* 15, 453–469. doi:10.5194/hess-15-453-2011
- 16 Miralles, D.G., Jiménez, C., Jung, M., Michel, D., Ershadi, A., McCabe, M.F., Hirschi, M.,
17 Martens, B., Dolman, A.J., Fisher, J.B., Mu, Q., Seneviratne, S.I., Wood, E.F., Fernández-
18 Prieto, D., 2016. The WACMOS-ET project - Part 2: Evaluation of global terrestrial
19 evaporation data sets. *Hydrol. Earth Syst. Sci.* 20, 823–842. doi:10.5194/hess-20-823-2016
- 20 Mu, Q., Zhao, M., Running, S.W., 2011. Improvements to a MODIS global terrestrial
21 evapotranspiration algorithm. *Remote Sens. Environ.* 115, 1781–1800.
22 doi:10.1016/j.rse.2011.02.019
- 23 Mueller, B., Hirschi, M., Jimenez, C., Ciais, P., Dirmeyer, P.A., Dolman, A.J., Fisher, J.B., Jung,
24 M., Ludwig, F., Maignan, F., Miralles, D.G., McCabe, M.F., Reichstein, M., Sheffield, J.,
25 Wang, K., Wood, E.F., Zhang, Y., Seneviratne, S.I., 2013. Benchmark products for land
26 evapotranspiration: LandFlux-EVAL multi-data set synthesis. *Hydrol. Earth Syst. Sci.* 17,
27 3707–3720. doi:10.5194/hess-17-3707-2013
- 28 Mulder, J.P.M., 1985. Simulating Interception Loss Using Standard Meteorological Data, in:
29 Hutchison, B.A., Hicks, B.B. (Eds.), *The Forest-Atmosphere Interaction*. pp. 177–196.
- 30 Ol’dekop, E.M., 1911. On evaporation from the surface of river basins. *Trans. Meteorol. Obs.* 4,
31 200.
- 32 Pearce, A.J., Rowe, L.K., 1981. Rainfall interception in a multi-storied, evergreen mixed forest:
33 estimates using Gash’s analytical model. *J. Hydrol.* 49, 341–353. doi:10.1016/S0022-
34 1694(81)80018-2
- 35 Pike, J.G., 1964. The estimation of annual run-off from meteorological data in a tropical climate.
36 *J. Hydrol.* 2, 116–123. doi:10.1016/0022-1694(64)90022-8
- 37 Porporato, A., Daly, E., Rodriguez-Iturbe, I., 2004. Soil water balance and ecosystem response
38 to climate change. *Am. Nat.* 164, 625–632. doi:10.1086/521238
- 39 Ruane, A.C., Goldberg, R., Chryssanthacopoulos, J., 2015. Climate forcing datasets for
40 agricultural modeling: Merged products for gap-filling and historical climate series

- 1 estimation. *Agric. For. Meteorol.* 200, 233–248. doi:10.1016/j.agrformet.2014.09.016
- 2 Savenije, H.H.G., 2004. The importance of interception and why we should delete the term
3 evapotranspiration from our vocabulary. *Hydrol. Process.* 18, 1507–1511.
4 doi:10.1002/hyp.5563
- 5 Schlesinger, W.H., Jasechko, S., 2014. Transpiration in the global water cycle. *Agric. For.*
6 *Meteorol.* 189–190, 115–117. doi:10.1016/j.agrformet.2014.01.011
- 7 Schreiber, P., 1904. About the relationship between the precipitation and the water management
8 of the river in Central Europe. *Meteorology* 21, 441–452.
- 9 Scott, R., Koster, R.D., Entekhabi, D., Suarez, M.J., 1995. Effect of a Canopy Interception
10 Reservoir on Hydrological Persistence in a General Circulation Model. *J. Clim.* 8, 1917–
11 1922. doi:10.1175/1520-0442(1995)008<1917:EOACIR>2.0.CO;2
- 12 Senay, G.B., Bohms, S., Singh, R.K., Gowda, P.H., Velpuri, N.M., Alemu, H., Verdin, J.P.,
13 2013. Operational Evapotranspiration Mapping Using Remote Sensing and Weather
14 Datasets: A New Parameterization for the SSEB Approach. *J. Am. Water Resour. Assoc.*
15 49, 577–591. doi:10.1111/jawr.12057
- 16 Shuttleworth, W.J., 1993. Evaporation, in: *Handbook of Hydrology*. McGraw-Hill, New York, p.
17 4.1-4.53.
- 18 Sutanto, S.J., 2015. Global transpiration fraction derived from water isotopologue datasets. *J.*
19 *Tek. Hidraul.* 6, 131–146.
- 20 Taylor, K.E., 2001. Summarizing multiple aspects of model performance in a single diagram. *J.*
21 *Geophys. Res.* 106, 7183–7192.
- 22 University of East Anglia Climatic Research Unit, Harris, I.C., Jones, P.D., 2014. CRU TS3.22:
23 Climatic Research Unit (CRU) Time-Series (TS) Version 3.22 of High Resolution Gridded
24 Data of Month-by-month Variation in Climate (Jan. 1901- Dec. 2013). NCAS Br. Atmos.
25 Data Cent. 24 Septemb. doi:10.5285/18BE23F8-D252-482D-8AF9-5D6A2D40990C
- 26 Von Hoyningen-Huene, J., 1981. Die Interzeption des Niederschlags in Landwirtschaftlichen
27 Pflanzenbeständen. *Arbeitsbericht Dtsch. Verband für Wasserwirtschaft und Kult.*
28 (Braunschweig DVWK).
- 29 Wang-erlandsson, L., Bastiaanssen, W.G.M., Gao, H., Jägermeyr, J., Senay, G.B., Dijk, A.I.J.M.
30 Van, Guerschman, J.P., Keys, P.W., Gordon, L.J., Savenije, H.H.G., 2016. Global root zone
31 storage capacity from satellite-based evaporation. *Hydrol. Earth Syst. Sci.* 20, 1459–1481.
32 doi:10.5194/hess-20-1459-2016
- 33 Wang-Erlandsson, L., Bastiaanssen, W.G.M., Gao, H., Jägermeyr, J., Senay, G.B., van Dijk,
34 A.I.J.M., Guerschman, J.P., Keys, P.W., Gordon, L.J., Savenije, H.H.G., 2016. Global root
35 zone storage capacity from satellite-based evaporation. *Hydrol. Earth Syst. Sci. Discuss.* 1–
36 49. doi:10.5194/hess-2015-533
- 37 Wang-Erlandsson, L., Van Der Ent, R.J., Gordon, L.J., Savenije, H.H.G., 2014. Contrasting roles
38 of interception and transpiration in the hydrological cycle - Part 1: Temporal characteristics
39 over land. *Earth Syst. Dyn.* 5, 441–469. doi:10.5194/esd-5-441-2014
- 40 Wang, D., 2012. Evaluating interannual water storage changes at watersheds in Illinois based on

1 long-term soil moisture and groundwater level data. *Water Resour. Res.* 48.
2 doi:10.1029/2011WR010759

3 Wei, Z., Yoshimura, K., Wang, L., Miralles, D., Jasechko, S., Lee, X., 2017. Revisiting the
4 contribution of transpiration to global terrestrial evapotranspiration. *Am. Geophys. Union.*
5 doi:10.1002/2016GL072235

6 Yang, D., Sun, F., Liu, Z., Cong, Z., Lei, Z., 2006. Interpreting the complementary relationship
7 in non-humid environments based on the Budyko and Penman hypotheses. *Geophys. Res.*
8 *Lett.* 33, 1–5. doi:10.1029/2006GL027657

9 Yang, H., Yang, D., Lei, Z., Sun, F., 2008. New analytical derivation of the mean annual water-
10 energy balance equation. *Water Resour. Res.* 44, W03410. doi:10.1029/2007WR006135

11 Zhang, L., Dawes, W.R., Walker, G.R., 2001. Response of Mean Annual Evapotranspiration to
12 Vegetationchanges at Catchment Scale. *Water Resour.* 37, 701–708.

13 Zhang, L., Hickel, K., Dawes, W.R., Chiew, F.H.S., Western, A.W., Briggs, P.R., 2004. A
14 rational function approach for estimating mean annual evapotranspiration. *Water Resour.*
15 *Res.* 40, WR002710. doi:10.1029/2003WR002710

16 Zhang, L., Potter, N., Hickel, K., Zhang, Y., Shao, Q., 2008. Water balance modeling over
17 variable time scales based on the Budyko framework – Model development and testing. *J.*
18 *Hydrol.* 360, 117–131. doi:10.1016/j.jhydrol.2008.07.021

19 Zhu, Z., Bi, J., Pan, Y., Ganguly, S., Anav, A., Xu, L., Samanta, A., Piao, S., Nemani, R.R.,
20 Myneni, R.B., 2013. Global data sets of vegetation leaf area index (LAI)_{3g} and fraction of
21 photosynthetically active radiation (FPAR)_{3g} derived from global inventory modeling and
22 mapping studies (GIMMS) normalized difference vegetation index (NDVI_{3G}) for the
23 period 1981 to 2. *Remote Sens.* 5, 927–948. doi:10.3390/rs5020927

24

1 **Table 1-** Budyko equations developed by different researchers.

| Equation | Reference |
|--|------------------|
| $\frac{E_a}{P_a} = 1 - \exp(-\phi)$ | Schreiber [1904] |
| $\frac{E_a}{P_a} = \phi \tanh\left(\frac{1}{\phi}\right)$ | Ol'dekop [1911] |
| $\frac{E_a}{P_a} = \frac{1}{\sqrt{0.9 + \left(\frac{1}{\phi}\right)^2}}$ | Turc [1954] |
| $\frac{E_a}{P_a} = \frac{1}{\sqrt{1 + \left(\frac{1}{\phi}\right)^2}}$ | Pike [1964] |
| $\frac{E_a}{P_a} = \left[\phi \tanh\left(\frac{1}{\phi}\right) (1 - \exp(-\phi))\right]^{1/2}$ | Budyko [1974] |

2

1 **Table 2-** Summary of the interception and transpiration equations of Gerrits' model (Gerrits et al., 2009)

| Equation | Equation number | Description |
|---|-----------------|--|
| $E_{i,d} = \min(D_{i,d}, P_d)$ | (4) | $E_{i,d}$: daily interception (mm day ⁻¹), P_d : daily precipitation (mm day ⁻¹), $D_{i,d}$: the daily interception threshold (mm day ⁻¹) |
| $E_{i,m} = P_m(1 - \exp(-\phi_{i,m}))$ | (5) | $E_{i,m}$: monthly interception (mm month ⁻¹), P_m : monthly rainfall (mm month ⁻¹), $\phi_{i,m}$: a sort of aridity index for interception at monthly scale |
| $E_{i,a} = P_a(1 - 2\phi_{i,a}K_0(2\sqrt{\phi_{i,a}}) - 2\sqrt{\phi_{i,a}}K_1(2\sqrt{\phi_{i,a}}))$ | (6) | $E_{i,a}$: annual interception (mm year ⁻¹), P_a : annual rainfall (mm year ⁻¹), $\phi_{i,a}$: a sort of aridity index for interception at annual scale, K_0 and K_1 : the Bessel function of the first and second order, respectively |
| $E_{t,m} = \min(A + B(P_m - E_{i,m}), D_{t,m})$ | (7) | $E_{t,m}$: monthly transpiration (mm month ⁻¹), A : carry-over parameter (mm month ⁻¹), $D_{t,m}$: the transpiration threshold (mm month ⁻¹), B : slope of relation between monthly effective rainfall and monthly transpiration |
| $A = bS_{u,max}$ | (8) | b : constant coefficient, $S_{u,max}$: the maximum root zone storage capacity |
| $E_{t,a} = 2BP_a(\phi_{i,a}K_0(2\sqrt{\phi_{i,a}}) + \sqrt{\phi_{i,a}}K_1(2\sqrt{\phi_{i,a}}))$ $\left(\frac{A}{\kappa_n B} + 1 - \exp(-\phi_{t,a})\left(\frac{A}{\kappa_n B} + 1 + \phi_{t,a} - \frac{\phi_{t,a}}{B}\right)\right)$ | (9) | $E_{t,a}$: annual transpiration (mm year ⁻¹), $\phi_{t,a}$: an aridity index |
| $D_{i,d} = \min(S_{max}, E_{p,d})$ | (10) | S_{max} : the daily interception storage capacity (mm day ⁻¹) $E_{p,d}$: the daily potential evaporation, $E_{p,a}$: annual potential evaporation (mm year ⁻¹) |
| $S_{max} \approx C_{max} = 0.935 + 0.498LAI - 0.00575LAI^2$ | (11) | LAI: Leaf Area Index derived from remote sensing images |
| $\phi_{i,m} = \frac{D_{i,d}}{\beta}$ | (12) | β : scaling factor |
| $\beta = \frac{P_m}{E(n_{r,d} n_m)}$ | (13) | $E(n_{r,d} n_m)$: the expected number of rain days per month, $n_{r,d}$: the number of rain days per month, n_m : the number of days per month |
| $\phi_{i,a} = \frac{n_{r,d}D_{i,d}}{\kappa_m}$ | (14) | κ_m : scaling factor for monthly rainfall |
| $\kappa_m = \frac{P_a}{E(n_{r,m} n_a)}$ | (15) | $E(n_{r,m} n_a)$: the expected number of rain months per year, $n_{r,m}$: the number of rain months per year, n_a : the number of months per year |
| $B = 1 - \gamma + \gamma \exp(-\frac{1}{\gamma})$ | (16) | γ : time scale for transpiration |
| $\gamma = \frac{S_b}{D_{t,m}\Delta t_m}$ | (17) | S_b : the moisture content below which transpiration is restricted (mm). |
| $S_b = aS_{u,max}$ | (18) | a : constant coefficient |
| $D_{t,m} = 0$ for LAI < 0.1 $D_{t,m} = \frac{E_p}{n_a}(-0.21 + 0.7LAI^{0.5})$ for 0.1 ≤ LAI < 2.7 $D_{t,m} = \frac{E_p}{n_a}$ for LAI ≥ 2.7 | (19) | E_p : annual potential evaporation (for open water) (mm year ⁻¹) |
| $\phi_{t,a} = \frac{D_{t,m}}{\kappa_n}$ | (20) | κ_n : scaling factor for monthly net rainfall |
| $\kappa_n = \frac{P_{n,a}}{E(n_{nr,m} n_a)} = \frac{P_a - E_{i,a}}{E(n_{nr,m} n_a)}$ | (21) | $P_{n,a}$: annual net precipitation, $E(n_{nr,m} n_a)$: the expected number of net rain months per year |

Table 3- Comparison of mean annual evaporation estimated by Gerrits' model to Landflux-EVAL, STEAM and GLEAM through Average, RMSE, MBE and RE per land cover type. Negative MBE and RE show the Gerrits' model underestimates evaporation and vice versa. Average, RMSE and MBE are in mm year⁻¹ and RE is in %.

| Land cover | area | Gerrits | Landflux-EVAL | | | | STEAM | | | | GLEAM | | | |
|---|----------------------|---------|---------------|------|------|-----|-------|------|------|-----|-------|------|------|-----|
| | 1000 km ² | Avg. | Avg. | RMSE | MBE | RE | Avg. | RMSE | MBE | RE | Avg. | RMSE | MBE | RE |
| Evergreen needleleaf forest | 5563 | 430 | 387 | 122 | +43 | +10 | 467 | 150 | -37 | -9 | 457 | 127 | -27 | -6 |
| Evergreen broadleaf forest | 11778 | 1367 | 1177 | 266 | +190 | +14 | 1129 | 345 | +238 | +17 | 1244 | 225 | +123 | +9 |
| Deciduous needleleaf forest | 2498 | 338 | 298 | 73 | +40 | +12 | 336 | 65 | +2 | +1 | 336 | 73 | +1 | 0 |
| Deciduous broadleaf forest | 1106 | 796 | 736 | 138 | +61 | +8 | 840 | 215 | -44 | -6 | 660 | 197 | +136 | +17 |
| Mixed forest | 13470 | 563 | 487 | 136 | +76 | +13 | 545 | 137 | +18 | +3 | 527 | 131 | +35 | +6 |
| Shrublands ¹ | 29542 | 203 | 259 | 96 | -57 | -28 | 262 | 123 | -59 | -29 | 253 | 91 | -51 | -25 |
| Savannas ² | 18846 | 695 | 739 | 148 | -44 | -6 | 737 | 186 | -42 | -6 | 705 | 154 | -10 | -1 |
| Grasslands | 21844 | 275 | 365 | 130 | -91 | -33 | 373 | 164 | -98 | -36 | 349 | 135 | -75 | -27 |
| Croplands | 12417 | 488 | 535 | 124 | -47 | -10 | 583 | 209 | -95 | -20 | 486 | 118 | +2 | 0 |
| Croplands and natural vegetation mosaic | 5782 | 687 | 696 | 157 | -9 | -1 | 702 | 175 | -15 | -2 | 663 | 158 | +24 | +3 |
| Global ³ | - | 443 | 469 | - | - | -6 | 475 | - | - | -7 | 462 | - | - | -4 |

¹including open and closed shrublands. ²including woody savannas and savannas. ³for overlapped pixels with 1.5°×1.5° resolution.

Table 4- Comparison of interception estimated by Gerrits' model to STEAM and GLEAM through Average, RMSE, MBE and RE per land cover type. Negative MBE and RE show the Gerrits' model underestimates evaporation and vice versa. Average, RMSE and MBE are in mm year⁻¹ and RE is in %.

| Land cover | Area | Gerrits | STEAM | | | GLEAM | | | | |
|---|----------------------|---------|-------|------|------|-------|------|------|------|-----|
| | 1000 km ² | Avg. | Avg. | RMSE | MBE | RE | Avg. | RMSE | MBE | RE |
| Evergreen needleleaf forest | 5563 | 145 | 204 | 70 | -58 | -40 | 127 | 58 | +18 | +12 |
| Evergreen broadleaf forest | 11778 | 452 | 499 | 120 | -47 | -10 | 340 | 130 | +111 | +25 |
| Deciduous needleleaf forest | 2498 | 104 | 156 | 56 | -53 | -51 | 29 | 76 | +74 | +72 |
| Deciduous broadleaf forest | 1106 | 179 | 299 | 145 | -120 | -67 | 80 | 117 | +99 | +55 |
| Mixed forest | 13470 | 172 | 220 | 59 | -48 | -28 | 127 | 66 | +45 | +26 |
| Shrublands ¹ | 29542 | 69 | 116 | 63 | -47 | -68 | 64 | 64 | +5 | +7 |
| Savannas ² | 18846 | 162 | 246 | 107 | -84 | -52 | 107 | 79 | +55 | +34 |
| Grasslands | 21844 | 76 | 146 | 83 | -70 | -93 | 97 | 58 | -22 | -29 |
| Croplands | 12417 | 116 | 174 | 89 | -58 | -50 | 97 | 55 | +19 | +16 |
| Croplands and natural vegetation mosaic | 5782 | 166 | 243 | 108 | -77 | -46 | 112 | 89 | +54 | +33 |
| Global ³ | - | 128 | 183 | - | - | -44 | 109 | - | - | +15 |

¹including open and closed shrublands. ²including woody savannas and savannas. ³for overlapped pixels with 1.5°×1.5° resolution.

Table 5- Comparison of transpiration estimated by Gerrits’ model to STEAM and GLEAM through Average, RMSE, MBE and RE per land cover type. Negative MBE and RE show the Gerrits’ model underestimates evaporation and vice versa. Average, RMSE and MBE are in mm year⁻¹ and RE is in %.

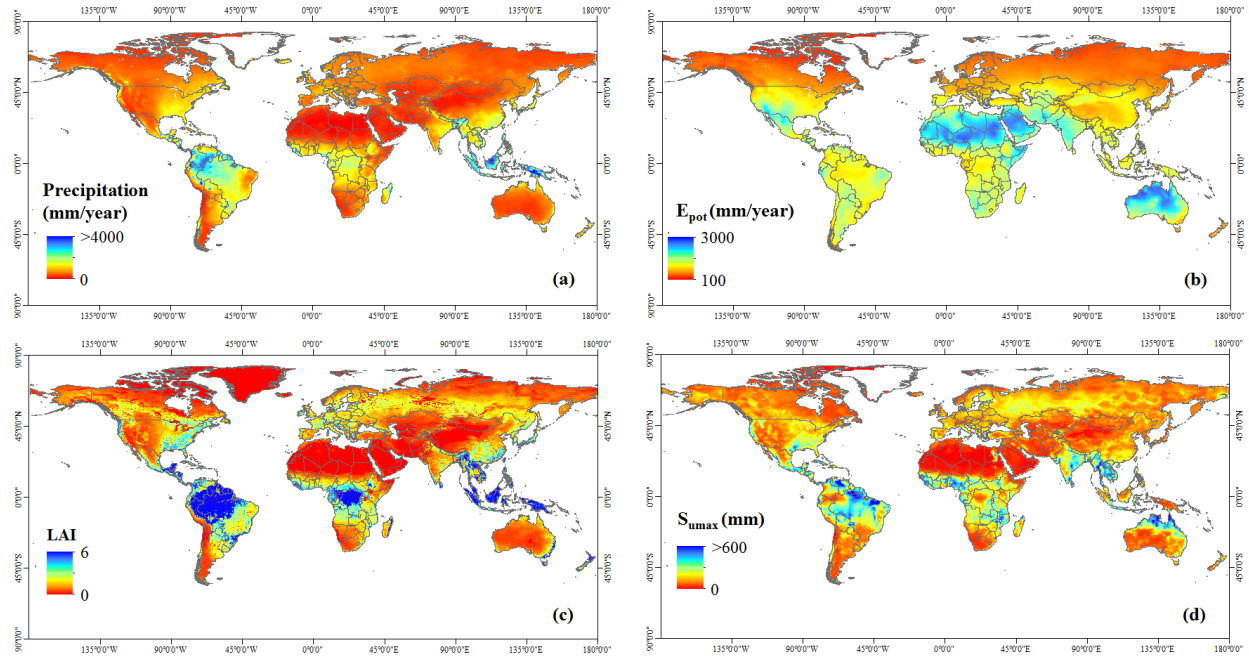
| Land cover | Area | Gerrits | STEAM | | | GLEAM | | | | |
|---|----------------------|---------|-------|------|------|-------|------|------|-----|-----|
| | 1000 km ² | Avg. | Avg. | RMSE | MBE | RE | Avg. | RMSE | MBE | RE |
| Evergreen needleleaf forest | 5563 | 284 | 222 | 122 | +63 | +22 | 259 | 100 | +25 | +9 |
| Evergreen broadleaf forest | 11778 | 915 | 619 | 347 | +296 | +32 | 890 | 163 | +25 | +3 |
| Deciduous needleleaf forest | 2498 | 234 | 177 | 82 | +57 | +24 | 261 | 71 | -21 | -12 |
| Deciduous broadleaf forest | 1106 | 617 | 538 | 192 | +79 | +13 | 570 | 120 | +47 | +16 |
| Mixed forest | 13470 | 390 | 305 | 147 | +85 | +22 | 363 | 114 | +27 | +7 |
| Shrublands ¹ | 29542 | 133 | 137 | 85 | +4 | +3 | 159 | 81 | -26 | -20 |
| Savannas ² | 18846 | 533 | 473 | 162 | +59 | +11 | 577 | 148 | -44 | -8 |
| Grasslands | 21844 | 199 | 214 | 109 | +15 | +7 | 233 | 93 | -34 | -17 |
| Croplands | 12417 | 372 | 393 | 131 | -20 | -5 | 371 | 90 | +1 | 0 |
| Croplands and natural vegetation mosaic | 5782 | 521 | 444 | 159 | +77 | +15 | 530 | 112 | -10 | -2 |
| Global ³ | - | 315 | 276 | - | - | +12 | 329 | - | - | -4 |

¹including open and closed shrublands. ²including woody savannas and savannas. ³for overlapped pixels with 1.5°×1.5° resolution.

Table 6 Comparison of mean annual evaporation estimated by Gerrits' model to Schreiber, Ol'dekop, Pike and Budyko through Average, RMSE, MBE and RE per land cover type. Negative MBE and RE show the Gerrits' model underestimates evaporation and vice versa. Average, RMSE and MBE are in mm year⁻¹ and RE is in %.

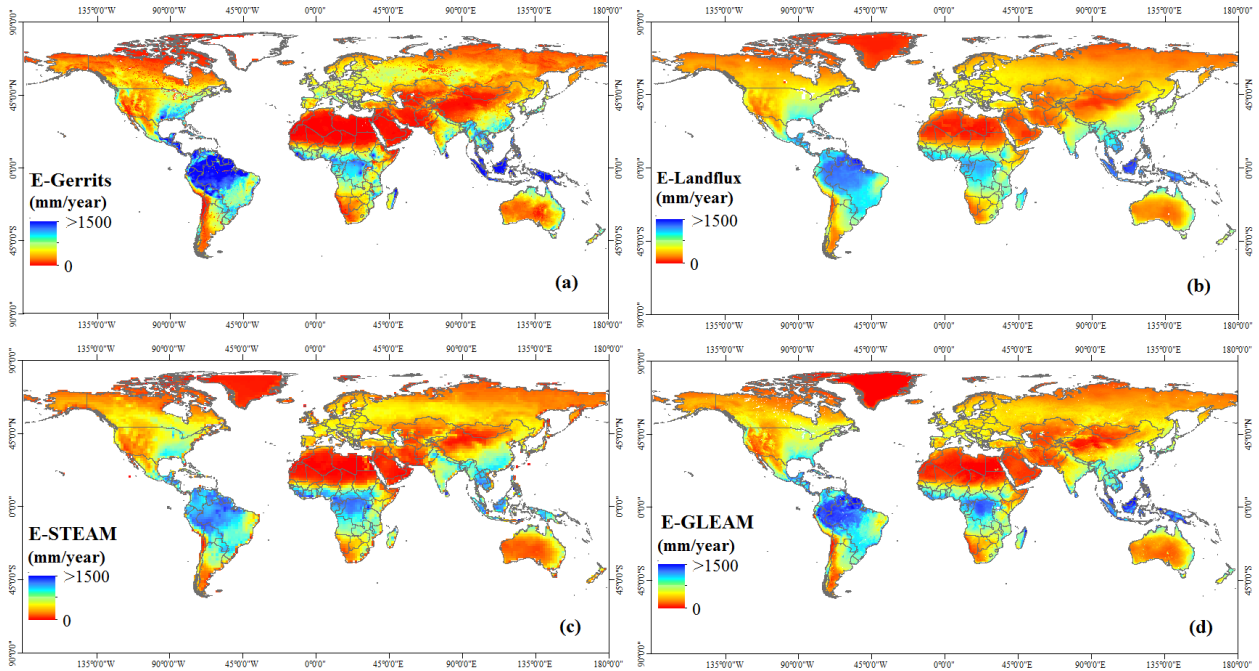
| Land cover | area | Gerrits | Schreiber | | | | Ol'dekop | | | | Pike | | | | Budyko | | | |
|---|---------------------|---------|-----------|------|------|-----|----------|------|------|-----|------|------|------|-----|--------|------|------|-----|
| | 1000km ² | Avg. | Avg. | RMSE | MBE | RE | Avg. | RMSE | MBE | RE | Avg. | RMSE | MBE | RE | Avg. | RMSE | MBE | RE |
| Evergreen-needleleaf forest | 5563 | 430 | 348 | 136 | +82 | +19 | 415 | 110 | +14 | +3 | 387 | 117 | +43 | +10 | 380 | 119 | +50 | +12 |
| Evergreen-broadleaf forest | 11778 | 1367 | 876 | 526 | +491 | +36 | 1065 | 355 | +301 | +22 | 991 | 419 | +375 | +27 | 966 | 443 | +401 | +29 |
| Deciduous-needleleaf forest | 2498 | 338 | 250 | 110 | +87 | +26 | 291 | 85 | +47 | +14 | 273 | 94 | +64 | +19 | 270 | 96 | +68 | +20 |
| Deciduous-broadleaf forest | 1106 | 796 | 636 | 22 | +161 | +20 | 727 | 120 | +69 | +9 | 687 | 152 | +109 | +14 | 680 | 160 | +117 | +15 |
| Mixed forest | 13470 | 563 | 420 | 185 | +142 | +25 | 506 | 134 | +56 | +10 | 470 | 150 | +92 | +16 | 461 | 156 | +101 | +18 |
| Shrublands ¹ | 29542 | 203 | 250 | 84 | -48 | -24 | 273 | 99 | -71 | -35 | 263 | 91 | -60 | -30 | 261 | 90 | -59 | -29 |
| Savannas ² | 18846 | 695 | 648 | 168 | +47 | +7 | 757 | 167 | -62 | -9 | 710 | 155 | -15 | -2 | 700 | 155 | -5 | -1 |
| Grasslands | 21844 | 275 | 346 | 134 | -71 | -26 | 372 | 152 | -98 | -36 | 359 | 141 | -85 | -31 | 358 | 140 | -84 | -31 |
| Croplands | 12417 | 488 | 502 | 154 | -14 | -3 | 566 | 181 | -78 | -16 | 538 | 164 | -50 | -10 | 533 | 162 | -45 | -9 |
| Croplands and natural vegetation mosaic | 5782 | 687 | 617 | 221 | +69 | +10 | 721 | 195 | -35 | -5 | 677 | 196 | -10 | -1 | 667 | 200 | -20 | -3 |
| Global ³ | - | 443 | 410 | - | - | +8 | 471 | - | - | -6 | 445 | - | - | 0 | 439 | - | - | +1 |

¹including open and closed shrublands. ²including woody savannas and savannas. ³for overlapped pixels with 1.5°×1.5° resolution.



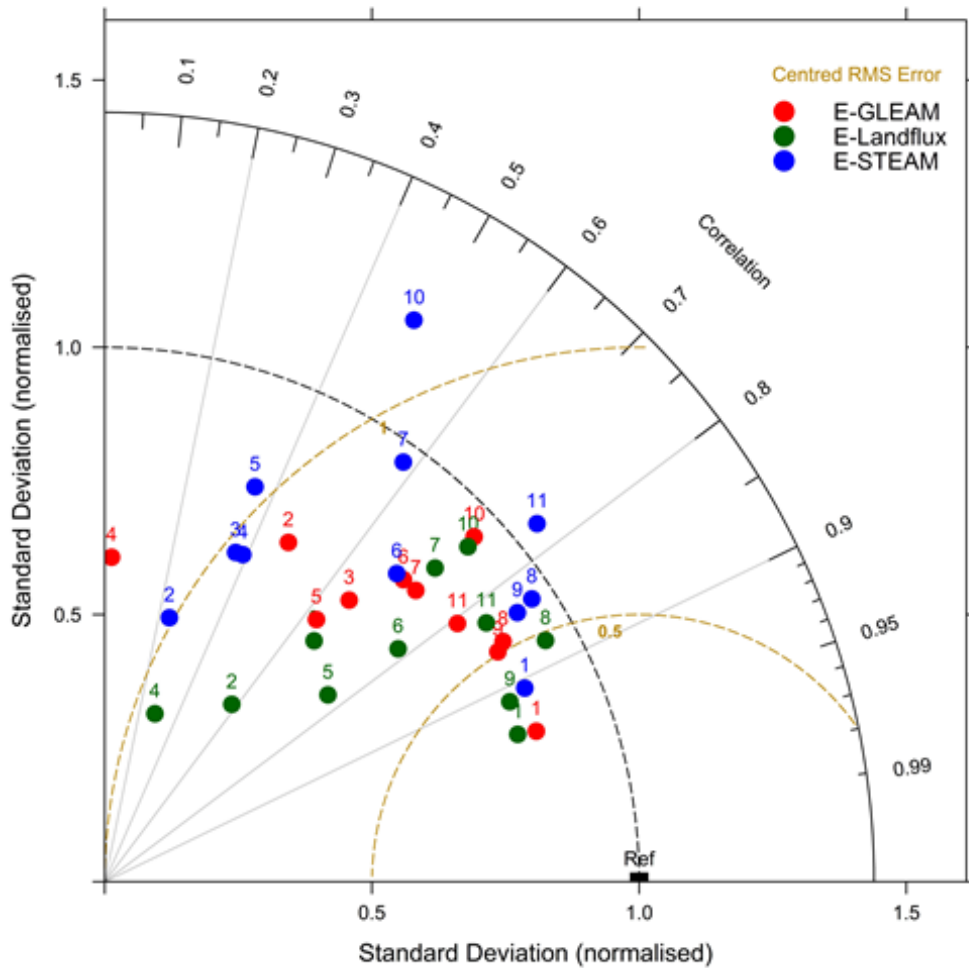
1

2 **Figure 1**— Mean annual of the applied data in the current study: (a) Precipitation (Ruane et al.,
 3 2015), (b) Potential evaporation (University of East Anglia Climatic Research Unit, 2014), (c)
 4 LAI (Zhu et al., 2013) and (d) $S_{u,max}$ (Wang-erlandsson et al., 2016).



1

2 **Figure 21**- Mean annual evaporation estimated by (a) Gerrits' model, (b) Landflux-EVAL, (c)
 3 STEAM and (d) GLEAM.

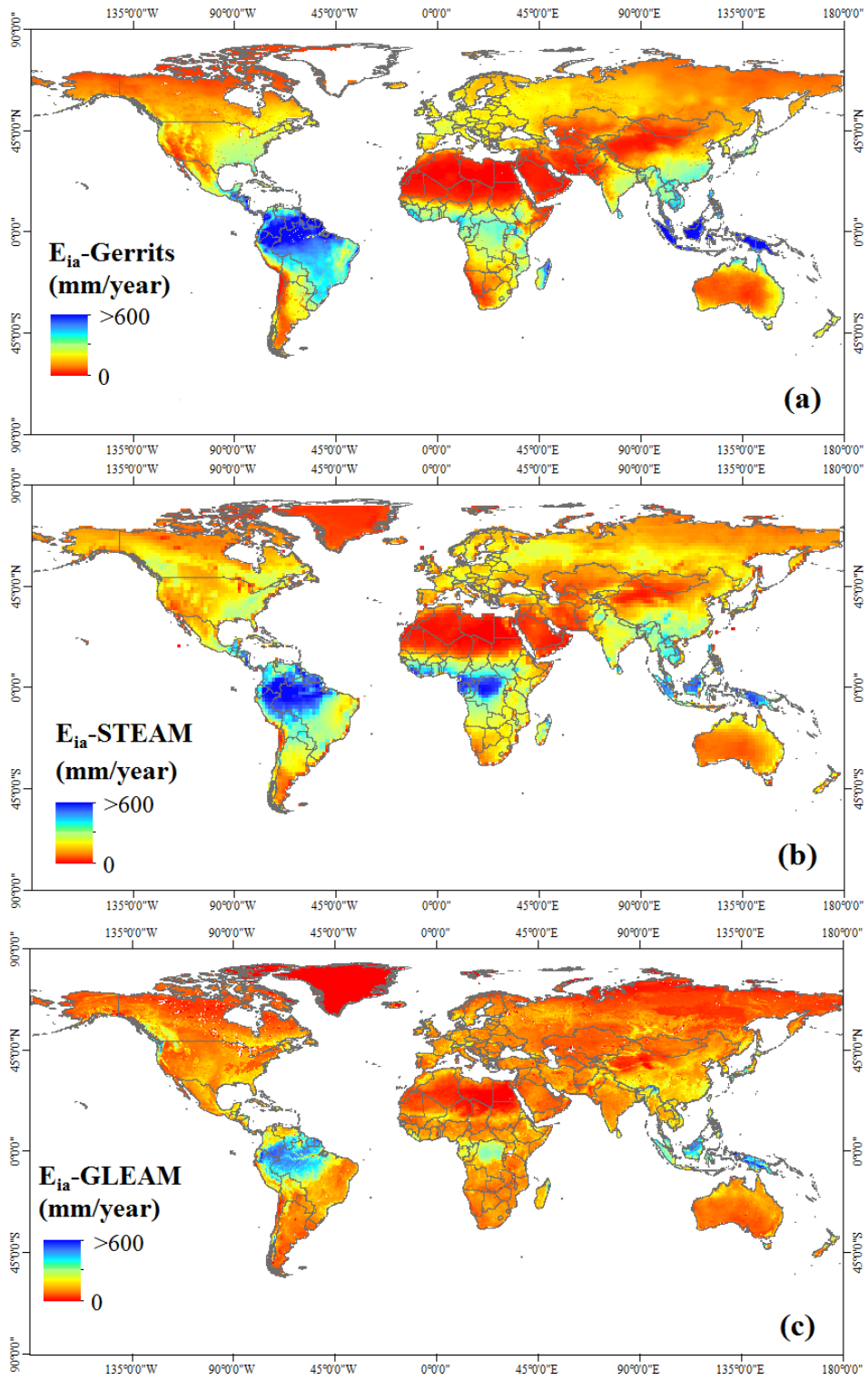


1

2 **Figure 32-** Taylor diagram for mean annual evaporation estimated by Gerrits' model in
 3 comparison to Landflux-EVAL (green circles), STEAM (blue circles) and GLEAM (red circles)
 4 for all data (No. 1), Evergreen Needleleaf Forest (No.2), Evergreen broadleaf forest (No. 3),
 5 Deciduous needleleaf forest (No. 4), Deciduous broadleaf forest (No. 5), Mixed Forest (No. 6),
 6 Shrublands (No. 7), Savannas (No. 8), Grasslands (No. 9), Croplands (No. 10) and Croplands and
 7 natural vegetation mosaic (No. 11).

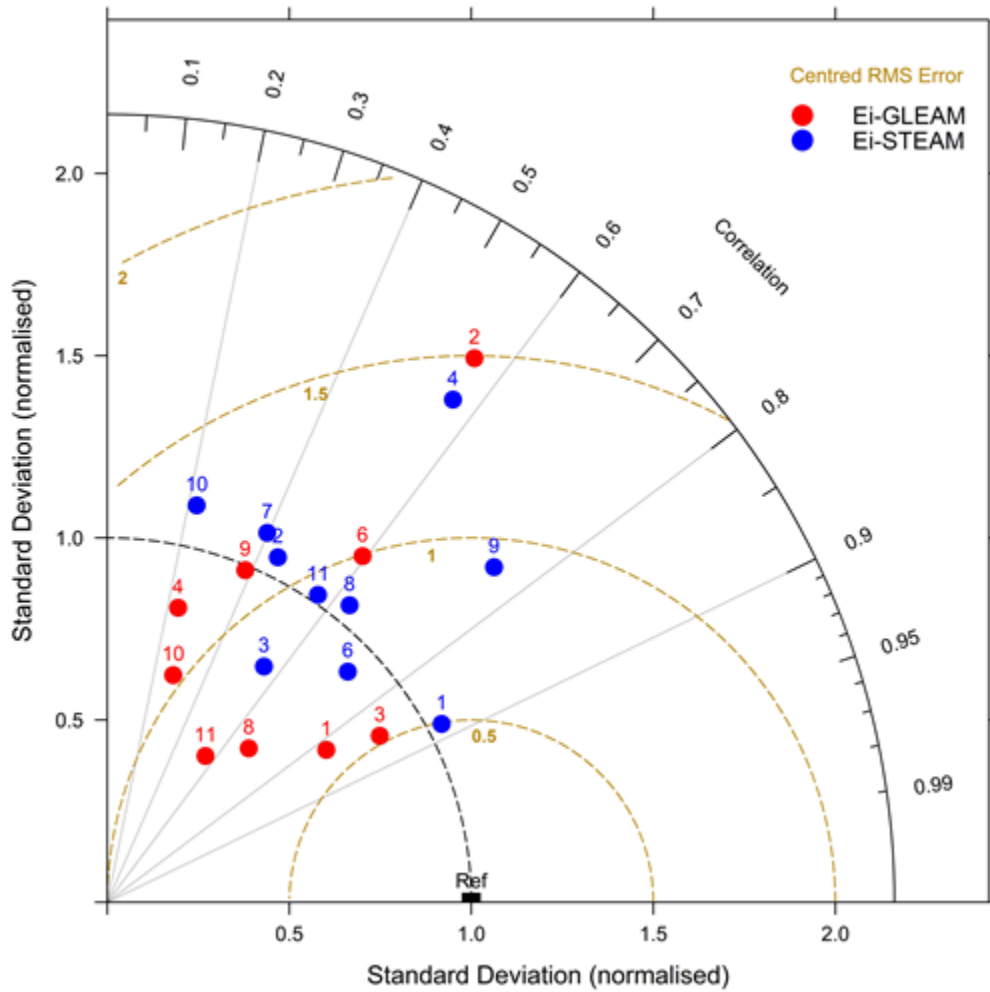
8

1



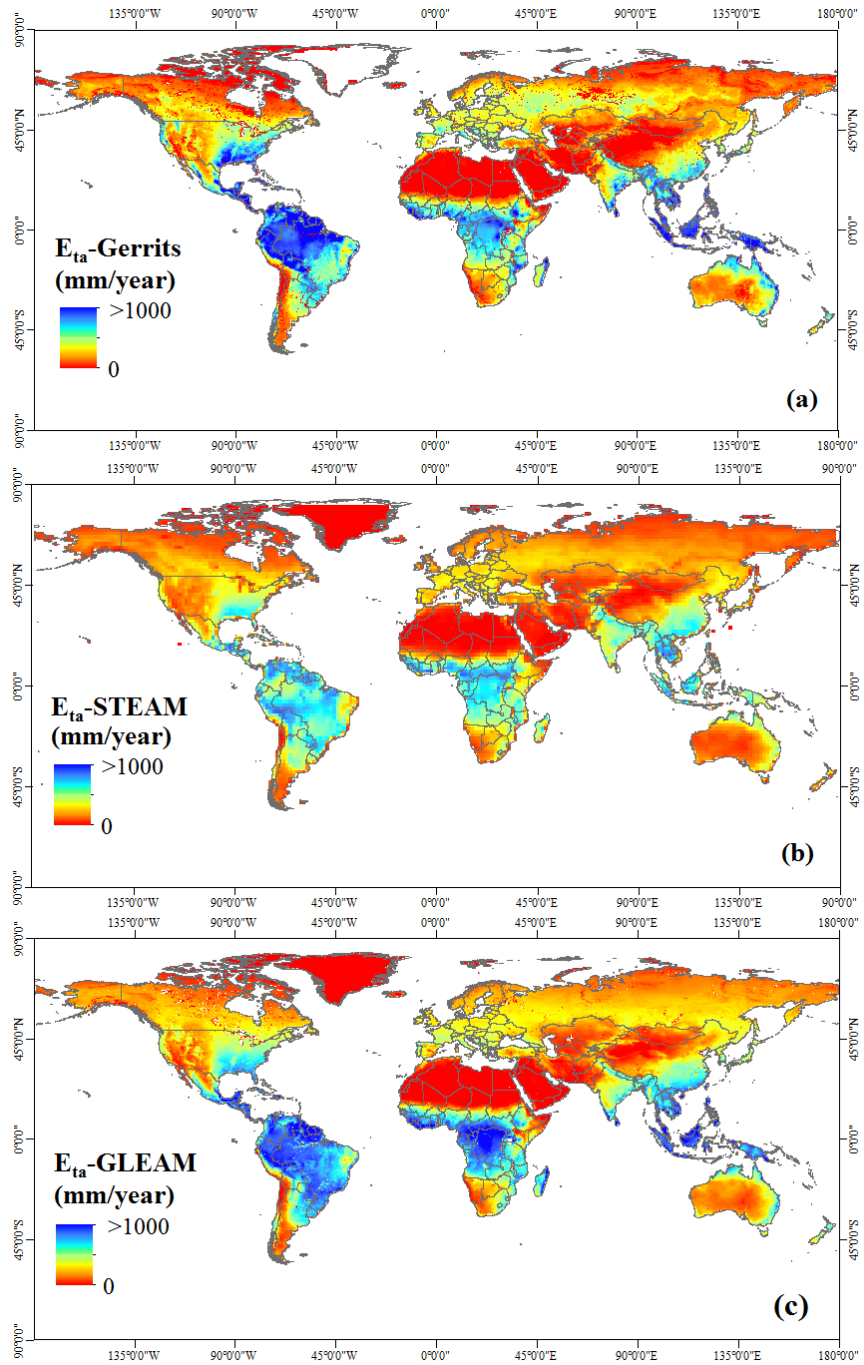
2

3 **Figure 43-** Simulated mean annual interception by (a) Gerrits' model and (b) STEAM and (c)
4 GLEAM.

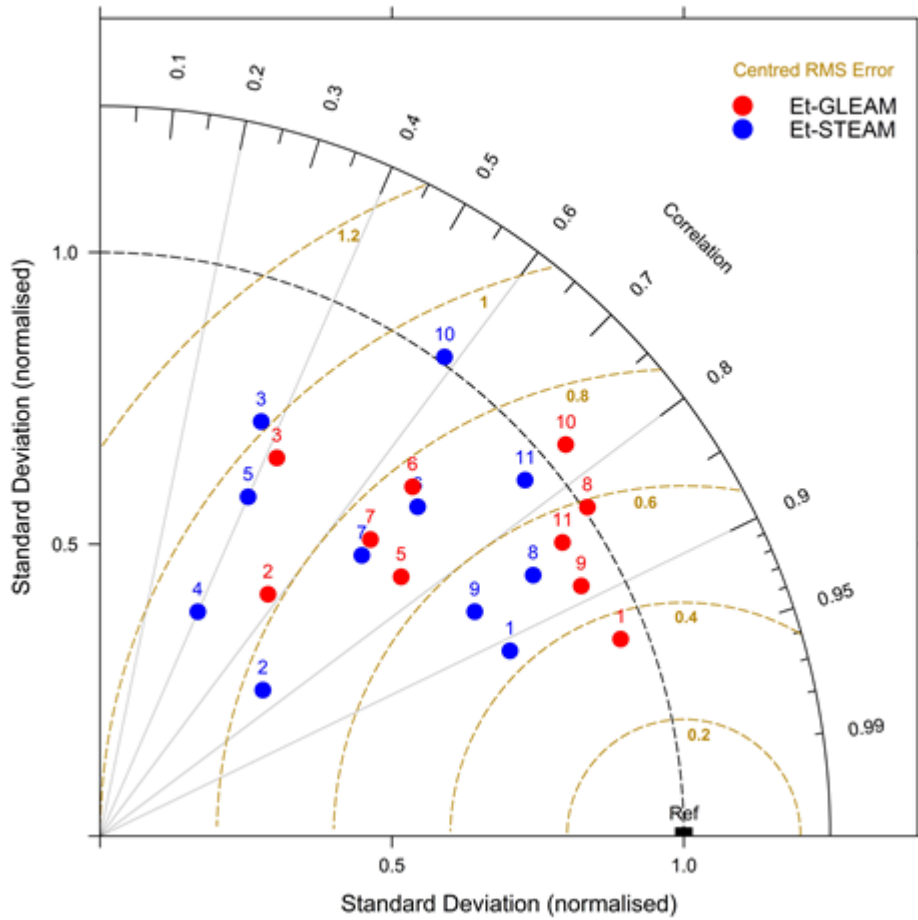


1
 2 **Figure 54-** Taylor diagram for mean annual interception estimated by Gerrits' model in
 3 comparison to STEAM (blue circles) and GLEAM (red circles) for all data (No. 1), Evergreen
 4 Needleleaf Forest (No.2), Evergreen broadleaf forest (No. 3), Deciduous needleleaf forest (No. 4),
 5 Deciduous broadleaf forest (No. 5), Mixed Forest (No. 6), Shrublands (No. 7), Savannas (No. 8),
 6 Grasslands (No. 9), Croplands (No. 10) and Croplands and natural vegetation mosaic (No. 11).

7



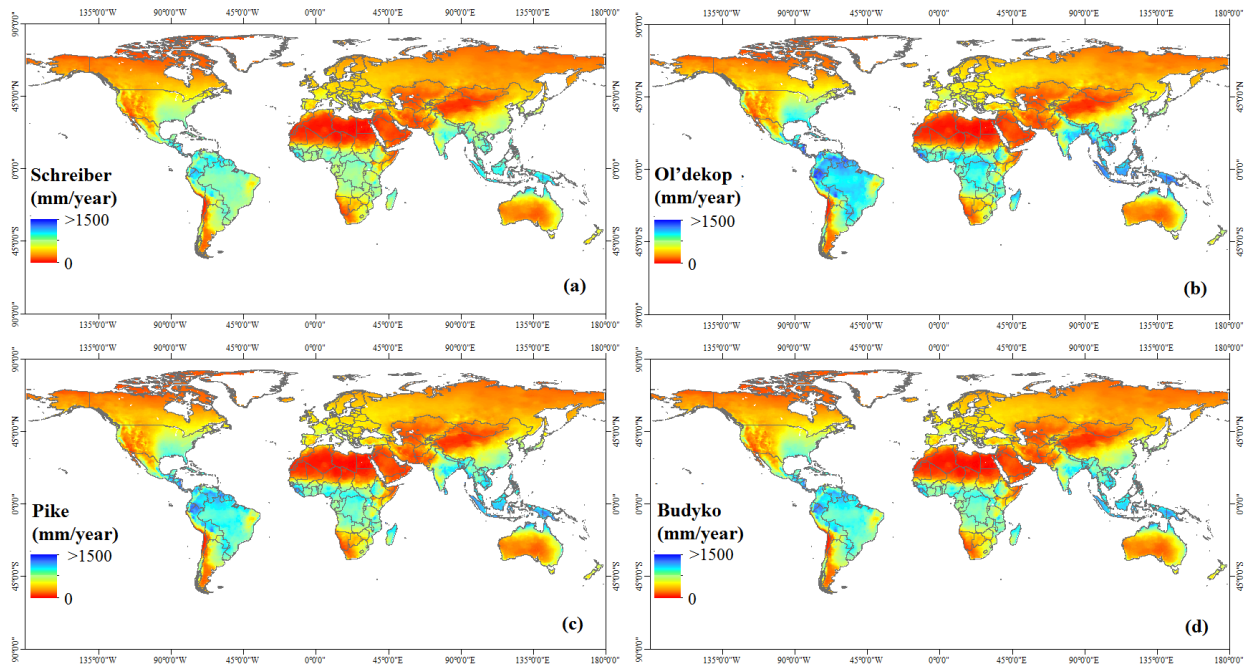
1
 2 **Figure 65-** Simulated mean annual transpiration by (a) Gerrits' model, (b) STEAM and (c)
 3 GLEAM.



1

2 **Figure 76-** Taylor diagram for mean annual transpiration estimated by Gerrits' model in
 3 comparison to STEAM (blue circles) and GLEAM (red circles) for all data (No. 1), Evergreen
 4 Needleleaf Forest (No.2), Evergreen broadleaf forest (No. 3), Deciduous needleleaf forest (No. 4),
 5 Deciduous broadleaf forest (No. 5), Mixed Forest (No. 6), Shrublands (No. 7), Savannas (No. 8),
 6 Grasslands (No. 9), Croplands (No. 10) and Croplands and natural vegetation mosaic (No. 11).

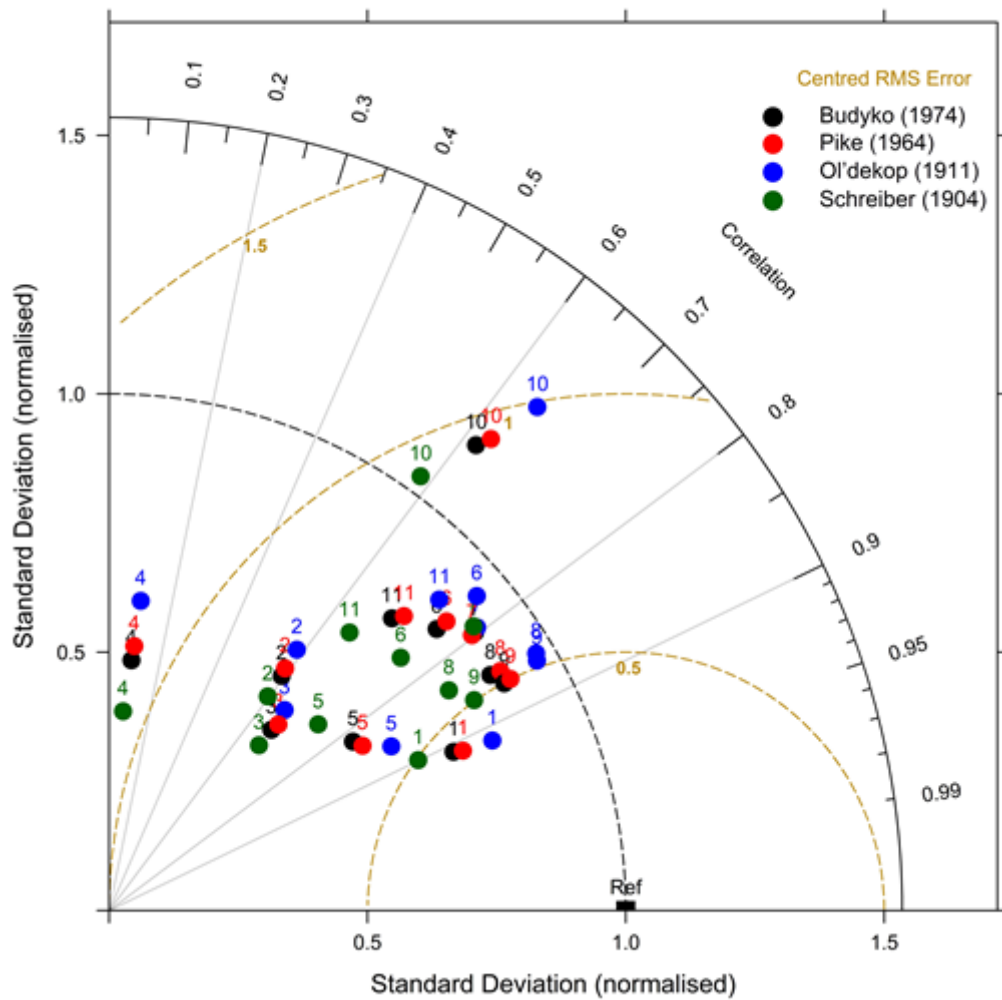
7



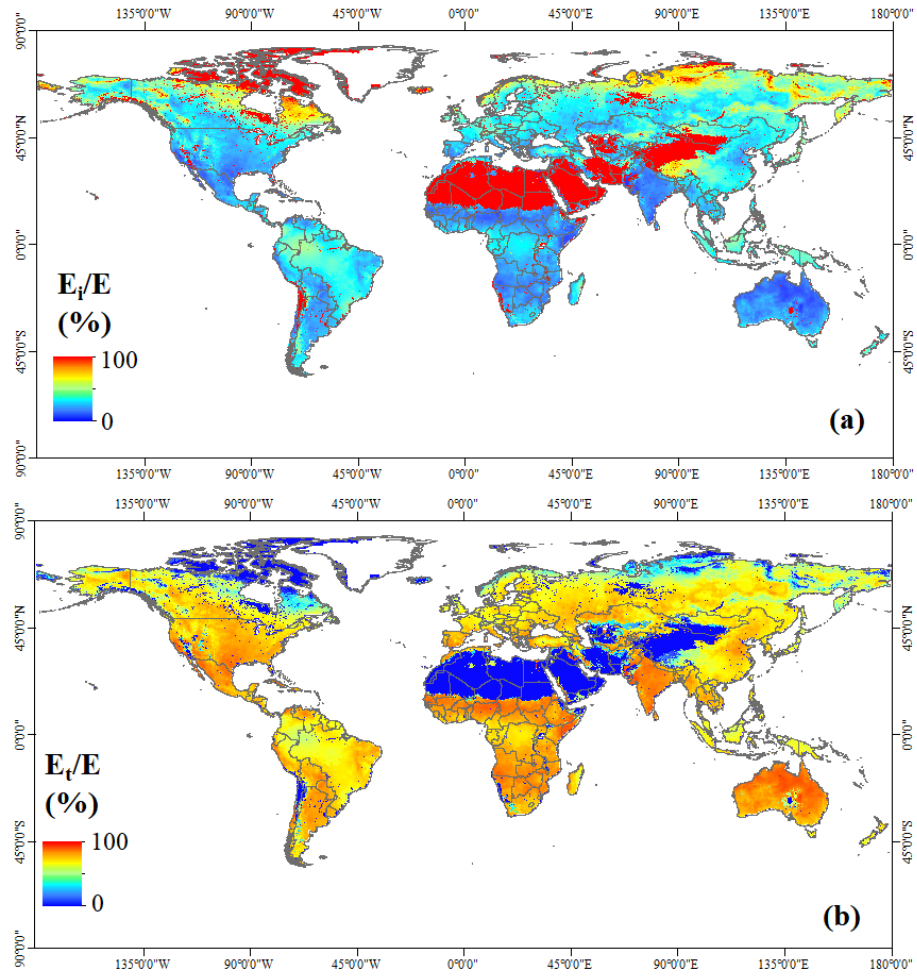
1

2 **Figure 8**—Global evaporation (mm year^{-1}) estimated by Budyko curves: (a) Schreiber (1904), (b)
 3 **Ol'dekop (1911), (c) Pike (1964), and (d) Budyko (1974).**

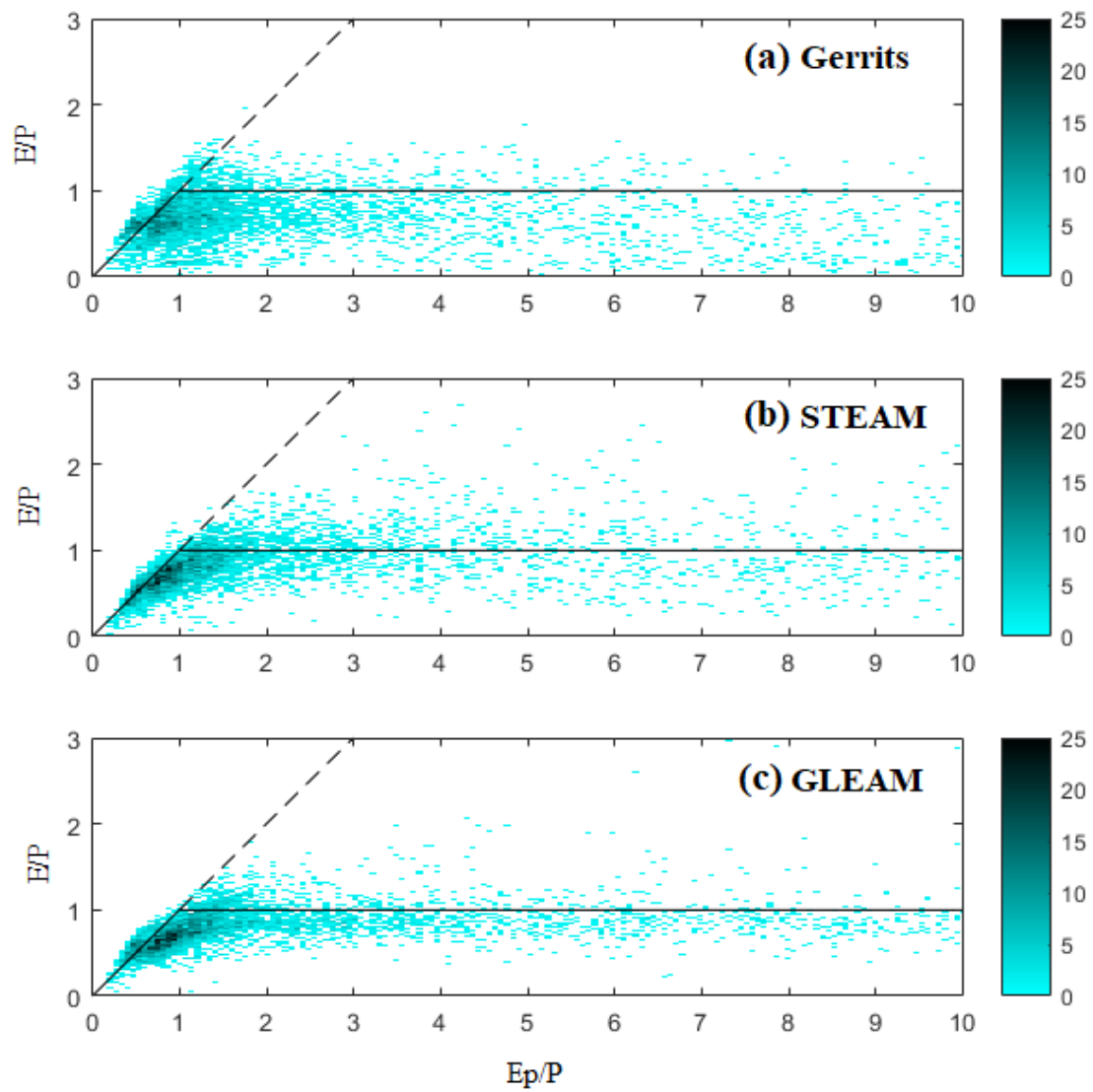
4



1
2 **Figure 9**– Taylor diagram for mean annual evaporation estimated by Gerrits’ model in
3 comparison to Schreiber (1904) (green circles), Ol’dekop (1911) (blue circles), Pike (1964) (red
4 circles), and Budyko (1974) (black circles) for all data (No. 1), Evergreen Needleleaf Forest
5 (No.2), Evergreen broadleaf forest (No. 3), Deciduous needleleaf forest (No. 4), Deciduous
6 broadleaf forest (No. 5), Mixed Forest (No. 6), Shrublands (No. 7), Savannas (No. 8), Grasslands
7 (No. 9), Croplands (No. 10) and Croplands and natural vegetation mosaic (No. 11).

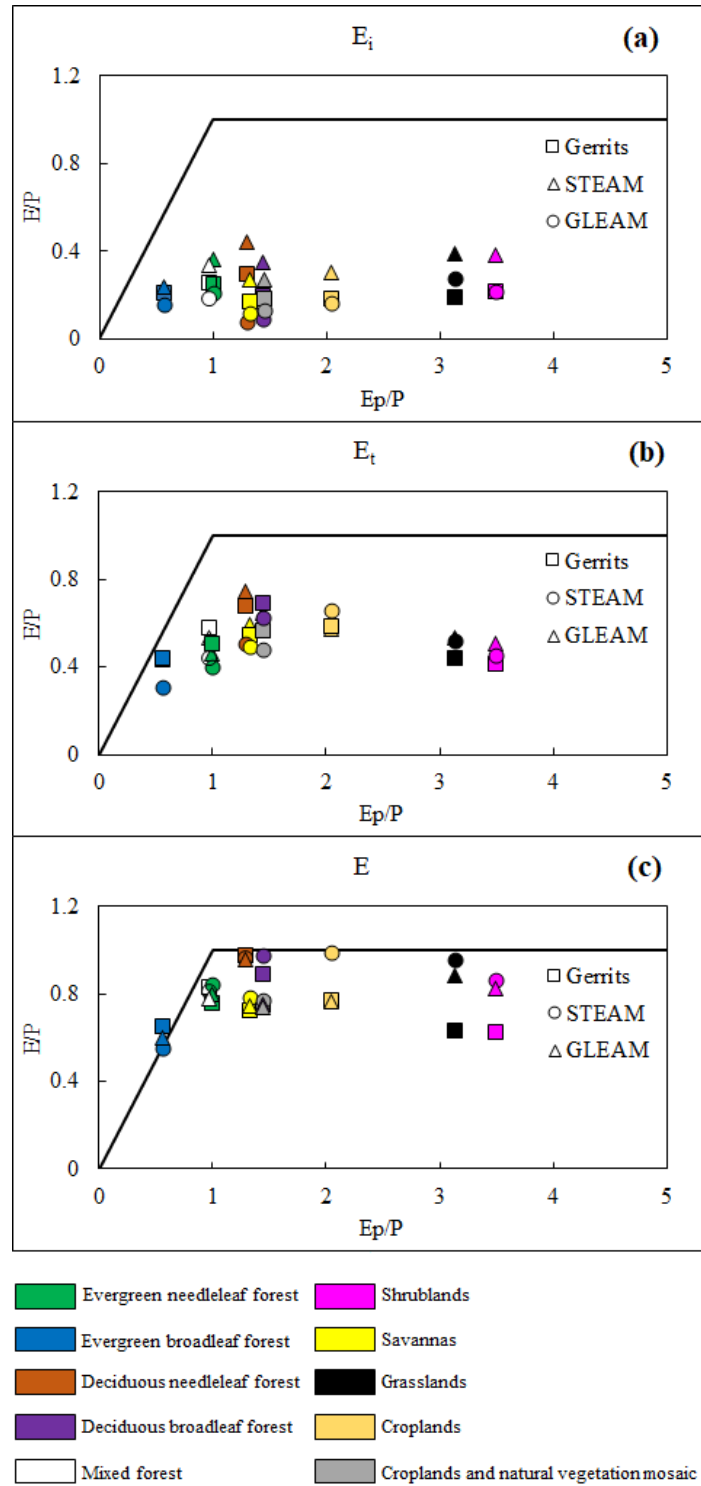


1
 2 **Figure 10—(a) Interception and (b) Transpiration ratio as a percentage of mean annual evaporation**
 3 **(Gerrits’ model).**



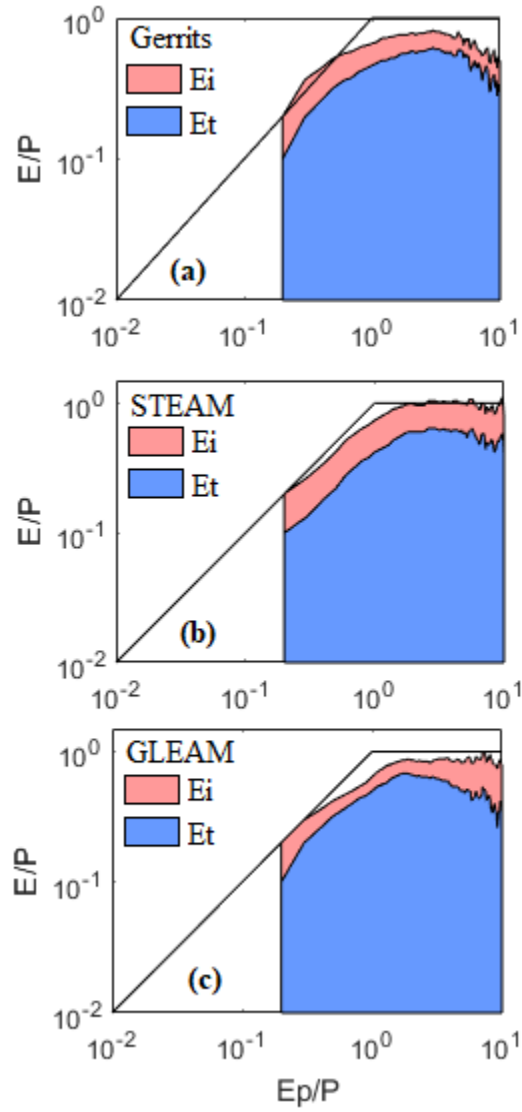
1

2 **Figure 7-** Density plot of $\frac{E}{p}$ versus $\frac{E_p}{p}$ for comparison between models within the Budyko
 3 framework. The legend shows the frequency of pixels.



1

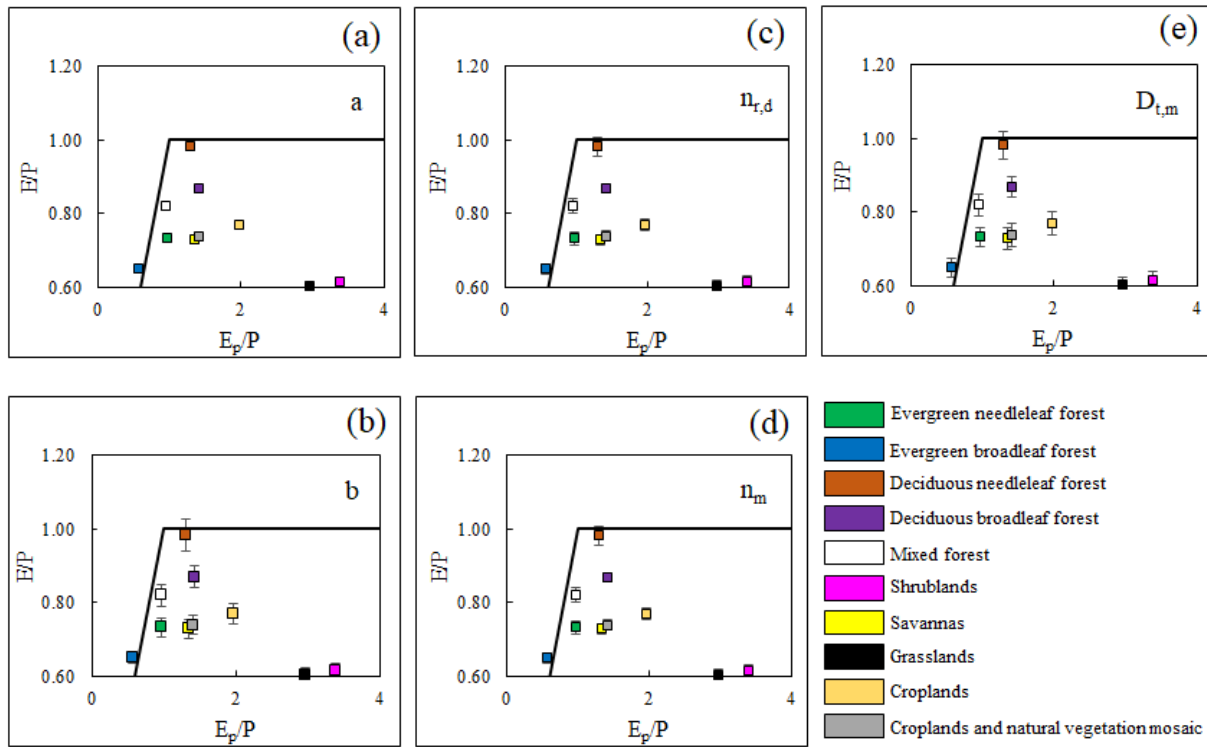
2 **Figure 8-** Comparison of interception (a), transpiration (b) and total evaporation (c) between
 3 models for each land cover within the Budyko framework.



1

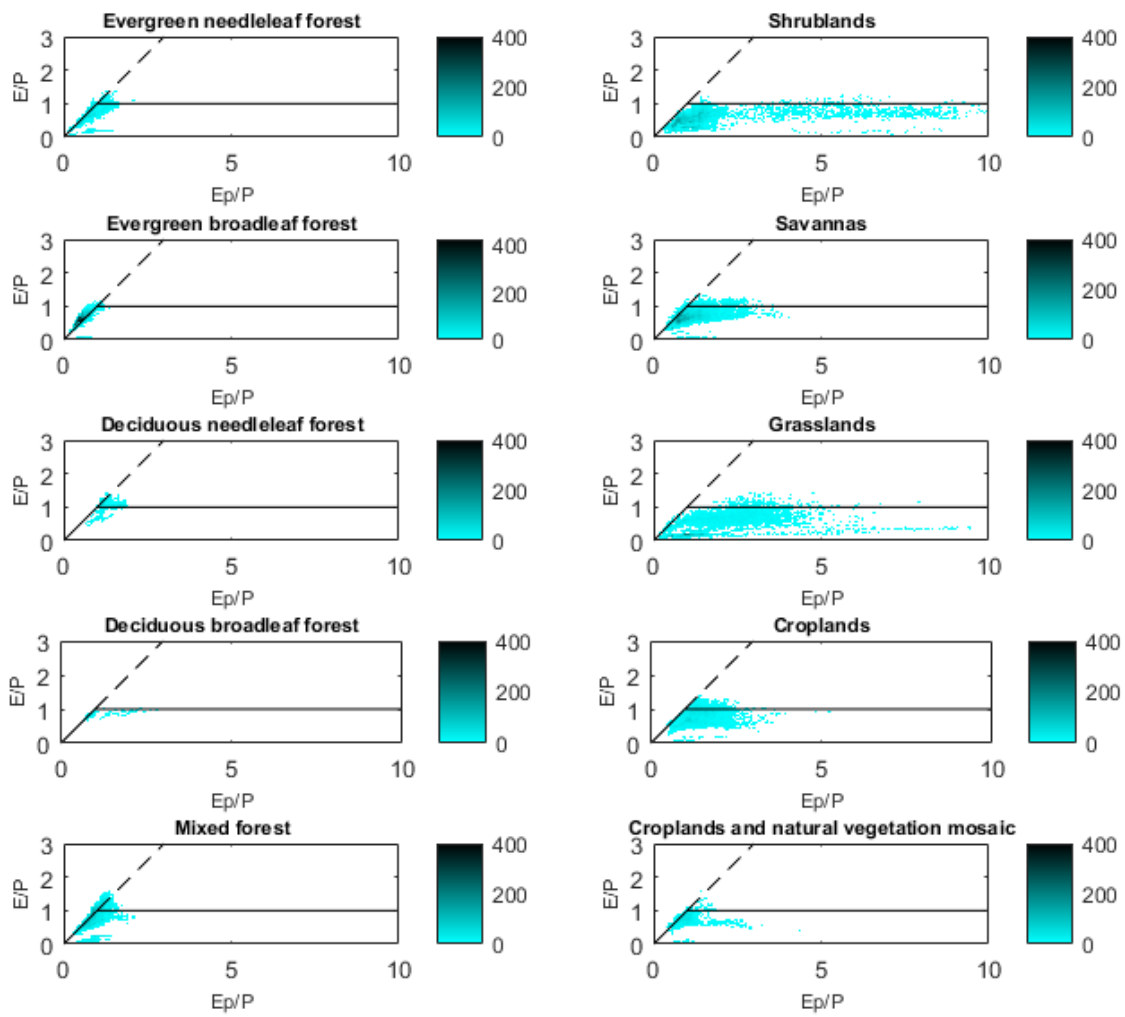
2 **Figure 9-** The distribution of $\frac{E_i}{P}$ and $\frac{E_p}{P}$ with respect to aridity for each model.

3



1

2 **Figure 10-** Sensitivity analysis of the model to 10% changes in (a) parameter a in equation 18 ,
 3 (b) parameter b in equation 8, (c) number of rain days $n_{r,d}$, (d) number of rain months n_{m} , and
 4 (e) transpiration threshold $D_{t,m}$.



1

2 **Figure 11-** Density plot of $\frac{E}{P}$ versus $\frac{E_p}{P}$ for each land cover.